

# Performance Comparison of Gallium Nitride (GaN) in DC-DC Converter Circuit

By

Maria Rahman

A THESIS SUBMITTED TO MACQUARIE UNIVERSITY

For the degree of

Master of Research

Department of Engineering

24 April, 2017



## **Abstract**

Solar power system is a free sources of sustainable power unlike fossil fuels, and inexhaustible. Converters can shift the level of voltage from one to another through switches. Which is very important for solar power system. Transistor plays a vital role in any converter circuit because the overall efficiency of a circuit depends on the switching losses. Transistor works as switch in a converter circuit.

In last few years it has been proven that Gallium Nitride (GaN) based switches have benefits over silicon switches. Using GaN technology reduces the cost of design and the construction of transistors. The GaN based transistor has the ability to operate at a high frequency with low switching power loss.

This study is based on a boost converter circuit, where three different transistor model were used to compare their output and efficiency. The output was measured based on simulation conducted on LTSpice platform. Then comes to a decision as to which transistor can give better performance.

## **Acknowledgements**

At first, I want to show my heartiest gratitude to my GOD, who has created me and this universe. My parents and family members who has supported and inspired me to work harder for my life.

I would like to acknowledge my academic supervisor Professor Michael Heimlich for accepting me as a research student under his supervision, and for the support and guidelines I have received during my study for the Master of Research.

I would like to thank Budhaditya Majumdar and Sudipta Chakraborty for helping me during the simulation work with LTSPice and thesis writing. Dr. Keith Imrie, Honorary Associate, Department of Engineering, provided copyediting and proofreading services as per the guideline provided by the university for research thesis writing.

Last but not the least, my gratitude to Macquarie University for giving me the opportunity to pursue my Master by Research in the Department of Engineering and giving a different experience for my life.

## **Statement of Originality**

The circuit used here for simulations taken from basic boost converter concept. The work of others has been acknowledged in the reference section.

This study result or any part of the study has not been used or submitted at any university or institution for any degree.

Maria Rahman

---

## List of Abbreviations and Symbols Used

$E_g$	Energy Gap
$E_{Br}$	Critical Electric Field
$V_s$	Saturation Velocity
$\mu$	Electron Mobility
HEMT	High Electron Mobility Transistor
HBT	Heterojunction Bipolar Transistor
LDMOS	Laterally Diffused MOSFET
RF	Radio Frequency
$V_{DS}$	Drain- Sourced Voltage
$I_D$	Drain Current
$V_F$	Forward Voltage
$I_F$	Forward Current
$v_s$	Saturated Drift Velocity

## Table of Contents

<b>Abstract .....</b>	<b>i</b>
<b>Acknowledgements .....</b>	<b>ii</b>
<b>Statement of Originality.....</b>	<b>iii</b>
<b>List of Acronyms Used.....</b>	<b>iv</b>
<b>List of Figures.....</b>	<b>vii</b>
<b>List of Tables .....</b>	<b>ix</b>
<b>Chapter 1: Introduction.....</b>	<b>1</b>
1.1 Transistors .....	1
1.2 LDMOS Transistor.....	3
1.3 Si Bipolar Transistor .....	4
1.4 GaN HEMT.....	5
1.5 Motivation of Work.....	5
1.6 Synopsis.....	6
<b>Chapter 2: Literature Review .....</b>	<b>8</b>
2.1 Introduction.....	8
2.2 Design Comparison for Converters.....	9
2.3 Power Loss in Converter .....	11
2.4 Efficiency for Converter.....	13
2.5 Material Properties .....	14
<b>Chapter 3: Analysis and Simulation Diagram .....</b>	<b>15</b>
3.1 Introduction to Basic Circuit .....	15
3.2 Simulation Circuit Diagram.....	16
3.3 List of Requirement and Parameters.....	18
3.4 Design Calculations and Selections .....	18
3.4.1 Duty Cycle Calculation .....	19
3.4.2 Switching Frequency Selection .....	19
3.4.3 Transistor Selection.....	20
3.4.4 Inductor Selection ( $L_1$ ) .....	21

3.4.5 Diode Selection ( $D_1$ ) .....	22
3.4.5 Capacitor Selection ( $C_1$ ) .....	22
<b>Chapter 4 : Circuit Descriptions and Simulations .....</b>	<b>24</b>
4.1 Requirements for the Design .....	25
4.2 Calculations and Circuit Diagram .....	25
4.2.1 Converter with NMOS .....	25
4.2.2 Converter with GaN .....	26
4.2.3 Converter with SiC .....	27
4.3 Output Graph of Different Transistor .....	28
<b>Chapter 5: Outcome and Results .....</b>	<b>35</b>
5.1 Output Voltage with Respect to Load .....	36
5.2 Efficiency with Load .....	37
5.3 Transistor Switching Turn-on Gate Voltage .....	39
5.4 Compare between GaN an SiC .....	41
<b>Chapter 6: Conclusion .....</b>	<b>42</b>
6.1 Summary of Work .....	43
6.2 Scope of Future Work .....	43
<b>Appendix .....</b>	<b>45</b>
<b>References .....</b>	<b>54</b>

## List of Figures

1.2.1 Schematic of an LDMOS [26] .....	3
1.3.1 Cross sections of an HBT [19].....	4
1.3.2 Evolution of cut-off frequency of different RF transistor [17] .....	4
1.4.1 Cross Section of an AlGaIn/GaN HEMT [20].....	5
2.2.1 Waveforms from switching gate and drain voltage [2] .....	9
2.2.2 Output voltage for the converter [2] .....	10
2.2.3 Efficiency of boost converter with respect to temperature [2].....	10
2.3.1 Experiment circuit to study power loss for converter [14] .....	11
2.3.2 (a) Waveform for proposed gate driver and (b), (c) Performance test circuit and turn on/turn off equivalent circuit for GaN [24] .....	12
2.3.3 Power loss for dc-dc boost converter for GaN (approximate) [2].....	13
2.4.1 Efficiency comparison for Si-based and GaN converters [8].....	13
2.4.2 Efficiency (a) and power loss (b) comparison for GaN and Si MOSFET [15] .....	14
2.5.1 Cross section of GaN [16] .....	14
3.1.1 Buck (a) and Boost (b) converter on and off state.....	16
3.2.1 Block diagram of boost converter .....	17
3.2.2 (a) On-state and (b) Off-state operation of a boost converter .....	17
3.2.3 Flow chart of working principal for the solar power .....	18
3.4.3.1 I-V characteristics curve for three transistors .....	20
3.4.5.1 Forward voltage characteristics for diode [71] .....	22
4.2.1 Converter with FDB2532.....	26
4.2.2 Converter with EPC2001 .....	27
4.2.3 Converter with C2M0025120D .....	28
4.3.1 Simulated output graph with 1- $\Omega$ load with FDB2532 .....	29
4.3.2 Simulated output graph with 1- $\Omega$ load with EPC2001 .....	29
4.3.3 Simulated output graph with 1- $\Omega$ load with C2M0025120D .....	30
4.3.4 Simulated output graph with 20- $\Omega$ load with FDB2532 .....	30
4.3.5 Simulated output graph with 20- $\Omega$ load with EPC2001 .....	31
4.3.6 Simulated output graph with 20- $\Omega$ load with C2M0025120D.....	31
4.3.7 Simulated output graph with 70- $\Omega$ load with FDB2532 .....	32



4.3.8 Simulated output graph with 70- $\Omega$ load with EPC2001 .....	32
4.3.9 Simulated output graph with 70- $\Omega$ load with C2M0025120D .....	33
4.3.10 FDB2532 output for 100 $\Omega$ .....	33
4.3.11 EPC2001 output for 100 $\Omega$ .....	34
4.3.12 C2M0025120D output for 100 $\Omega$ .....	34
5.1.1 Output voltage comparison for three transistors .....	37
5.2.1 Efficiency comparison of three transistors .....	39
5.3.1 Gate turn-on pulse voltage comparison .....	40

## List of Tables

1.1.1 Thermal properties of material [20].....	2
1.1.2 Material properties of semiconductor [20].....	2
3.3.1 List of required parameters for design .....	18
3.4.2 Switching frequency effect on properties.....	19
3.4.3.1 Switching transistor name and model number .....	20
3.4.3.2 Transistor parameters as per datasheet .....	21
4.1.1 Component parameters for the design.....	25
4.2.1 FDB2532 Supply voltage .....	26
4.2.2 EPC2001 Supply voltage .....	27
4.2.3 EPC2001 Supply voltage .....	28
5.1.1 Output and voltage measured with respect to different load .....	36
5.2.1 Efficiency for transistors.....	38

# Chapter 1

## Introduction

### 1.1 Transistors

The power transistor is a device that used as a switch in power electronics. Power transistor, especially the metal-oxide-semiconductor-field-effect transistor (MOSFET) has advantages for majority carrier device of achieving high operating frequency. The insulated gate bipolar transistor (IGBT) is recent in this field and its performance improving regularly with time. IGBT already replaces bipolar transistor in many areas of power electronics. However, for application below 200V, MOSFETs are the only choice as a switch. MOSFETs are majority carrier device where IGBTs are minority carrier. This has an effect on device performance as majority carrier charges faster than minority carrier devices.

Materials have long been a very important component in the field of semiconductors, GaN being considered one of the most ideal for microwave device fabrication with high power. This GaN also has high output power and high efficiency. The thermal management of GaN devices is also very good compared to other devices.

The power density for GaN is higher than for Si-based materials and thermal conductivity becomes a very important parameter for materials, because this determines how good heat dissipation will be for any device. Also important are the properties of dielectric and conductor loss for device efficiency.

Table 1.1.1 shows the density and related temperature properties for different materials.

Table 1.1.1: Thermal properties of materials [20].

Materials	Density (gm/cm <sup>3</sup> )	Heat (J/kg °C)
Gallium Nitride (GaN)	6.1	490
Silicon Carbide (SiC)	3.1	681
Au	19.32	126
AuSn	14.5	150
Cu	8.3	385

GaN has a bandgap of 3.2 eV, higher than other materials. The bandgap for materials is related to the amount of energy requires for shifting an electron from the valence band to the conduction band for a semiconductor. So this is very important for wide bandgap materials. GaN also has a  $2.5 \times 10^7$  cm/s saturation velocity, which exceeds the value needed to achieve high energy state. Table 1.1.2 shows the material properties comparison for materials,

Table 1.1.2: Material properties for semiconductor [20]

Properties	GaN	AlN	4H- SiC	Si	GaAs	InP
E <sub>g</sub> (eV)	3.4	6.2	3.2	1.12	1.43	1.35
E <sub>Br</sub> (MV/CM)	3.3	8.4	3.5	0.3	0.4	0.5
v <sub>s</sub>	2.5	2.16	2.0	1	1	1
( $\times 10^7$ cm/s)						

Considering  $E_{Br}$ , the critical electric field for the breakdown of semiconductors,  $v_s$ , the saturated drift velocity,  $E_g$ , the bandgap of the semiconductor

## 1.2 LDMOS Transistors

Laterally diffused metal oxide (LDMOS) semiconductor transistors were introduced around 20 years back as a replacement for bipolar transistors for Radio Frequency (RF) applications. In recent times, the development has reached the point where new opportunities are introduced, such as RF lighting and microwave cooking, and the frequency range has improved from 1 MHz to 4 GHz. In this emergence of new technology, development of semiconductor devices has many challenges. RF devices play a vital role in power amplifier designs. LDMOS has low intermodulation, higher gain and reduces the thermal effect of source inductance enabling. Figure 1.2.1 shows a cross section for an LDMOS transistor.

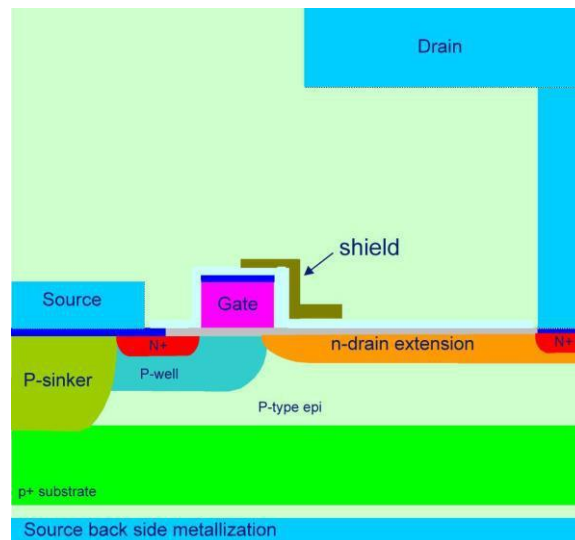


Figure 1.2.1: Schematic of an LDMOS [26]

LDMOS are voltage controlled devices, it been more than ten years semiconductor industry started using LDMOS as RF power technology. In the figure of the cross section of LDMOS, we can see the n+ region is connected to the back side with a metal bridge a p+ sinker and a highly conducting p+ substrate. The flow of current will go through drain from source to drain if the gate is positively biased inverting the laterally diffused p+ well.

The gate length has been reduced dramatically to increase the gain of the transistor. In terms of the reliability issues of LDMOS, special consideration must be given to the hot carrier degradation, where electrons and holes are trapped in the hot surface oxide due to the high electric field. There are some advantages of using high switching frequency, like reducing the cost of input and output

capacitances, increase the system performance and lowers the cost. So for designing the high frequency dc-dc converter circuit, LDMOS can be a very good option for frequency range

### 1.3 Si Bipolar Transistor

Bipolar transistors are able to employ vertical current transport. So through this wafer area can be used more efficiently and able to provide give high power density. In bipolar transistors, AlGaAs or GaAs has shown superior material properties compared to Si-based BJTs. Due to the high bandgap emitter and superior material the development of bipolar transistor was done. Si based bipolar transistors has enough maturity to operate RF-powered devices because of their intrinsic high power density and linearity.

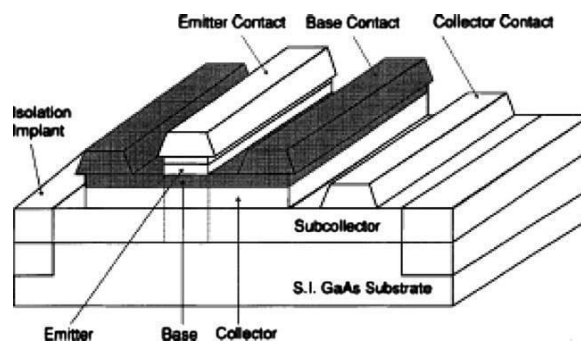


Figure 1.3.1: cross section of an HBT [19]

In between 1970 and 2000, RF electronics started using III-V transistors, while conventional Si bipolar transistors were available to use commercially. Since then the situation has been changed a lot and now SiGe HBTs are being used in RF applications.

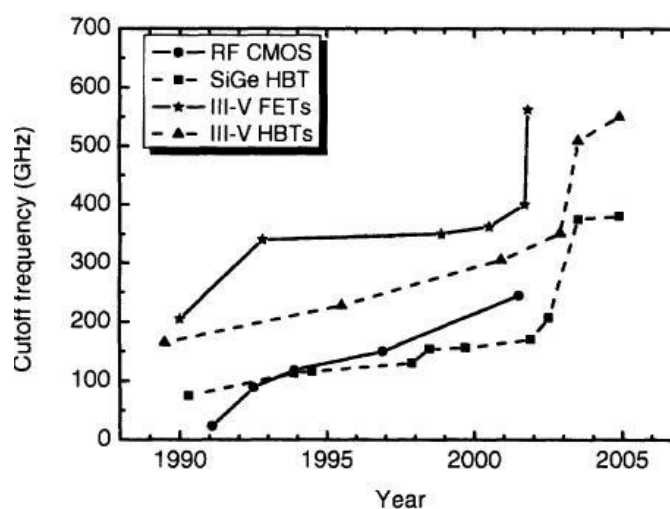


Figure 1.3.2: Evolution of cut- off frequency of different RF transistor [17]

From the figure, we can see the differences in the frequency limits of the Si-based transistors. It clearly shows their dramatic improvement with time. With respect to time, it has been improved dramatically, and has advantage in performance and cost. Mostly for applications operating in frequency up to 2.5 GHz, Si based HBT has cost advantage.

## 1.4 GaN HEMT

GaN can have the lowest dislocation density and this gives it a high epitaxial quality. GaN HEMTs are grown on a silicon substrate by Molecular Beam Epitaxy, using an RF plasma source [23]. To minimise the effect of lattice mismatch and thermal coefficient mismatch, a thin layer of aluminium nitride (AlN) layer is grown first. GaN has achieved better microwave noise performance than GaAs. Figure 1.4.1 shows a cross section of a GaN HEMT [20]

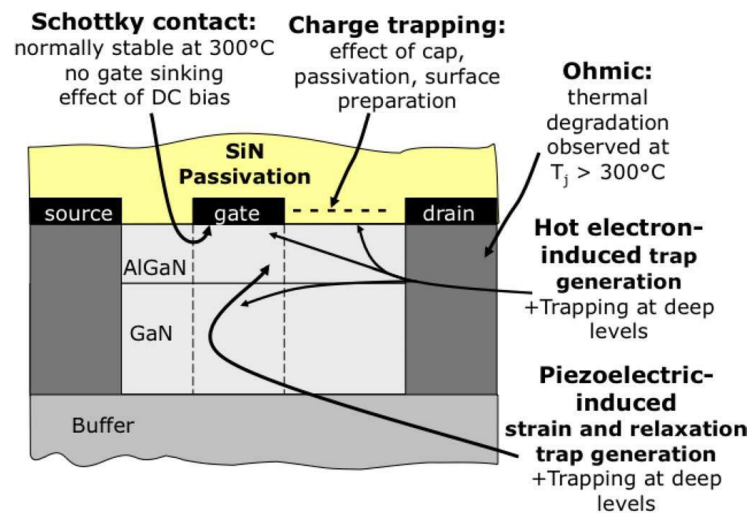


Figure 1.4.1: Cross section of an AlGaIn/ GaN HEMT [20]

The devices with GaN are half in size with compare to silicon-based devices. Here in term of high-efficiency GaN is considered more ideal when compare to silicon because of some physical limitations and realization of switch mode on Si-based MOSFETs. Another advantage of GaN HEMT is a body diode with it, which makes the gate charge lower than Si based MOSFET and this helps the GaN transistor to switch at higher frequency.

## 1.5 Motivation of Work

A basic DC- DC converter circuit does almost the same task that a regulator does. However, when it comes to the high frequency and high voltage, converters are more reliable than a regulator. Converters also help in term of thermal properties by producing less heat and power loss. The two basic converters are buck and boost converters. The main function of a buck converter is to step down

the voltage from the input to the output. This kind of switching converter which gives much better efficiency than a linear regulator.

Boost converters are used to get a higher voltage from lower voltage battery cells, especially in the case where the cells are limited but we need to get a higher voltage. For example in a car the voltage of nearly 417 cells is required but space is available for only 168 cells and there using a boost converter can give up to 500 V from a 202 V input. Also this converter help to use the entire energy of a battery which might get wasted as its low voltage is depleted. Both the buck and boost converter gives better efficiency than any other linear regulators without a step up of the current.

A recent study shows that using Gallium Nitride (GaN) has become widely popular for inverters. It has better switching modes at higher frequency and also allows a reducing the size of an inverter. Especially for high power density and using high frequency, this has become widely accepted. Now usually, for high-frequency devices, we need to consider the size and also the cost of production as well, GaN has become the only option. This study was conducted to check the performance of a GaN transistor in a basic boost converter and test how much better it can perform than to same wide band semiconductor SiC and NMOS.

Solar photovoltaic (PV) system has very large effect on the efficiency of converter. The research in the field of semiconductor has rapidly increased due to the growth of solar PV system. In today's use, most of appliances like DC motors, computing or communicating equipment are capable to run in DC power. A dc-dc converter allows to convert the power level up to or down according to the load. Therefore, dc-dc converter has very important role in this PV industry specially to integrate solar power directly into loads. For example, to use in houses where the load requirement is less, a very good efficient converter will be cost effective and compact. A high-frequency power switching can result high frequency and reliability. So this study will show performances of transistors as a switch for a dc-dc boost converter and how see their performance.

## **1.6 Synopsis**

This study of performance comparison was conducted in the period of nine months, mostly focusing on selecting a transistors for dc-dc boost converter circuit. Starting with Chapter 1 for introduction of this thesis study, in Chapter 2 a short background study description is presented, mostly the research areas and which has shown that GaN has better performance for efficiency. In Chapter 3 the a introduction to the converter circuit used to run the tests is given. This circuit has three different versions with different transistors. in Chapter 4 the results found from simulation are



given. The simulations were run by LTSPice and the outputs figures have shown. Chapter 5 discusses the final outcome reached from the simulations and chapter 6 gives the conclusions of the study.

# Chapter 2

## Literature Review

### 2.1: Introduction:

GaN has long been considered for power FETs and getting a lot of attention for its performance. In the field of power electronics a converter can work for both small voltage and high voltage. The cost is a point of discussion but as the power loss is less and it has high switching frequency, cost compare to the efficiency considered as a trade-off. The primary focus of research area was to reduce cost and improve the efficiency of the converter, and to increase the switching frequency that will reduce the size and components of the converter. In another term the transistor has low switching loss can have higher switching frequency.

GaN devices have this characteristic of lower switching loss [2] and this characteristic allows this to operate at a high switching frequency. In the last few years, it has been proven that, to increase the efficiency of a PV system Gallium Nitride based switches are having better benefits instead of other silicon switches. Using Gallium Nitride technology also reduces the cost of the design and construction of the power electronics to be used in solar power converters. The current trend of using a micro-inverter which includes single power optimisation of each solar panel improves the installation and safety with minimisation of the cost of solar energy.

## 2.2 Design Comparisons for Converters

In the design of a high-efficiency, compact and step down power stage based on the dual active bridge, GaN transistors were used to measure the performance [1]. At microwave frequencies, GaN transistors have proven excellent performances. From the study of an experiment with a typical boost converter [2] using a GaN HEMT as a switching transistor, up to eighty-five percent efficiency was achieved. It was also found the power loss was less than for the other transistor switches and the switching loss was reduced. For this study waveforms were measured shown in Figure 2.1.1

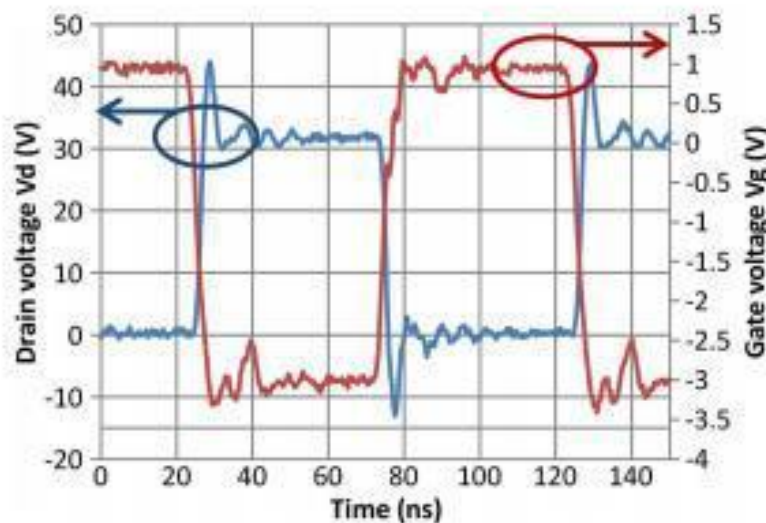


Figure 2.2.1: Waveforms from switching gate and drain voltages [2]

These waveform were obtained by measuring different gate and drain voltages. The switching frequency was 10 MHz during the measurement. The load resistor was kept at 75  $\Omega$ s and duty cycle was 0.5. A basic converter circuit with GaN as switching transistor was used.

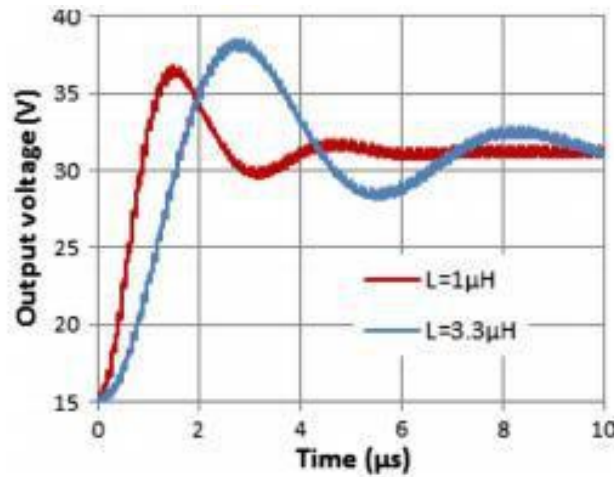


Figure 2.2.2: Output voltages for the converter [2]

When measuring the waveform, two different inductors were used for the converter circuit and the average current found to be 0.9 A. The efficiency also was measured for the converter within different temperature and shown in Figure 2.1.3.

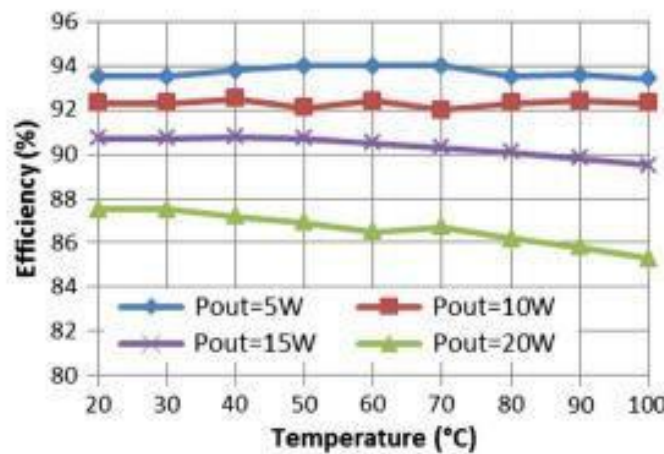


Figure 2.2.3: Efficiency of boost converter as a function of temperatures [2]

The measured efficiency was found to be above 80%, which was measured to check the potentiality of GaN converters for high-speed RF applications at the ambient temperature of 100°C [2]. One common problem can be found at switching started for the dc-dc converter is huge current and overshoot of output voltage, which might be found to damage the inductor and also create instability [3], [4], [5]. In that case, an external capacitor can regulate the soft starter but this will incur some additional cost and some damages to external components. Another study of

miniaturisation of dc-dc converter shows that a high switching frequency can reduce the size of the converter [6].

The author of [12] shows that, even if the frequency goes over 5 MHz GaN HEMTs show better efficiency, hence achieving efficiency at a higher frequency is a challenge for dc-dc converters. GaN has a low gate charge with a low gate-to-source voltage. A GaN can give faster switching speed due to its small physical size and low parasitic capacitance. Another of its characteristics is zero source-to-drain recovery charge [13].

The heating effect is another important issue for high- power GaN HEMTs. A temperature effect is observed in source-drain, at the end of the source and drain contacts. So heat is actually generated there where many FETs have dropped heat [21]. But still, GaN is cheaper than Si and has better ratings and a smaller in size. Though SiC and GaN have almost the same properties, GaN shows superior performance for power devices [22], but thermal conductivity becomes an issue for GaN for showing poor properties. However, when it comes to lattice mismatch or thermal mismatch, GaN has zero mismatches but SiC has 3.5% mismatch [22].

### 2.3 Power Loss in Converter

During the study for power loss for both Si based and GaN converters, only the turn-off loss was calculated in [14] and this shows that the magnetising inductance is important to analyse the losses. An experimental circuit is shown below.

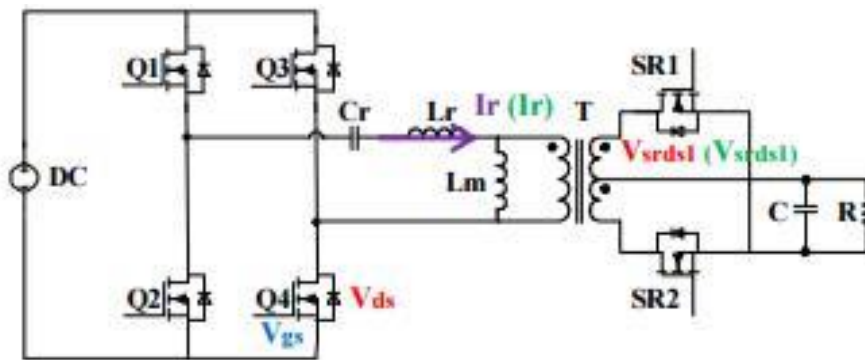


Figure 2.3.1: Experiment circuit to study power loss for converter [14]

Figure 2.2.1 is an example of the converter circuit that was studied for the loss calculations [14]. GaN and Si MOSFETs have shown completely different diode mechanisms when the reverse

recovery charge was zero. The GaN transistor model used for the study is the same as will be used for the current study, so it will be easier to compare the performance.

From the study of [24] found a switching speed for GaN has found 9 ns for turn on and 43.2 ns for turn off while for Si-based power MOSFET it was 50 ns and 62 ns so the switching speed for GaN is faster. The experimental circuit is shown here in Figure 1.4.2.

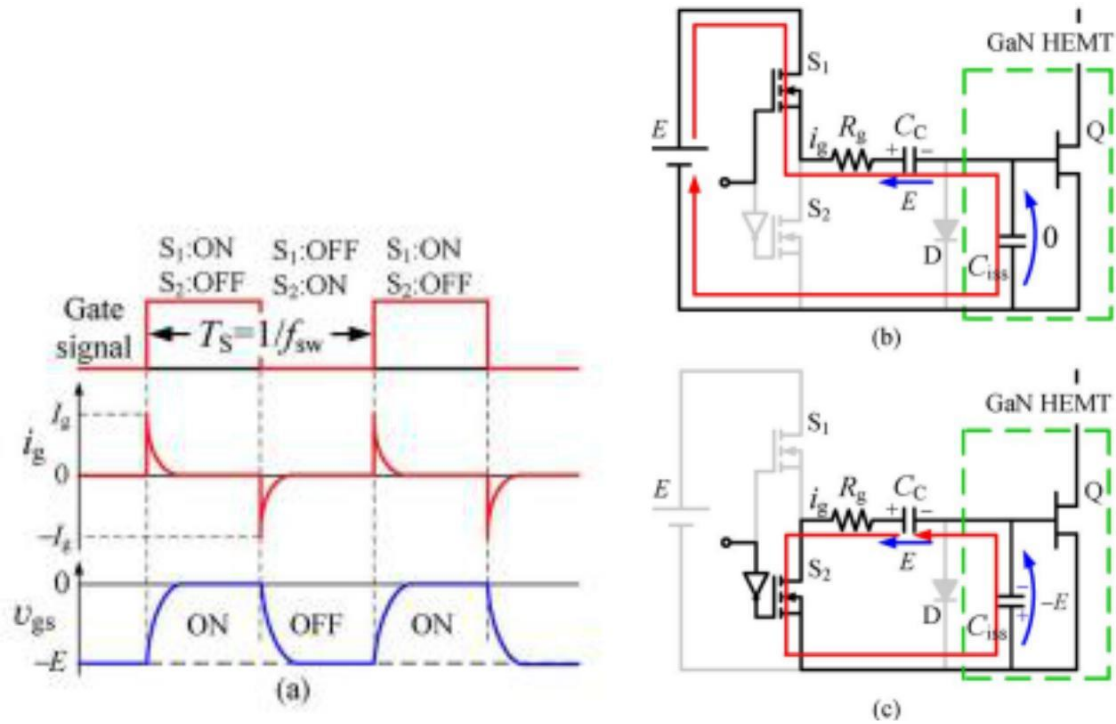


Figure 2.3.2: (a) Waveform for proposed gate driver and (b), (c) Performance test circuit and turn on/turn off equivalent circuit for GaN [24]

However, the turn-off time is higher than turn-on time, which might be caused by electrons trapped on the surface during turn-on state of a GaN HEMT; the current collapse is increased by decreasing the gate-source voltage for this HEMT.

From the power-loss calculations, study shows that GaN switching FETs have better performance, showing a low power loss [2]. A figure is in Figure 2.2.3. For switching loss, on-off and off-on times were measured. The author of [7], mentioned that for GaN transistors has the pull up-down resistance of the gate driver and the amplitude of the gate driver output voltage, can determine the capability effect of a power device, but in the different operating condition, the role is different.

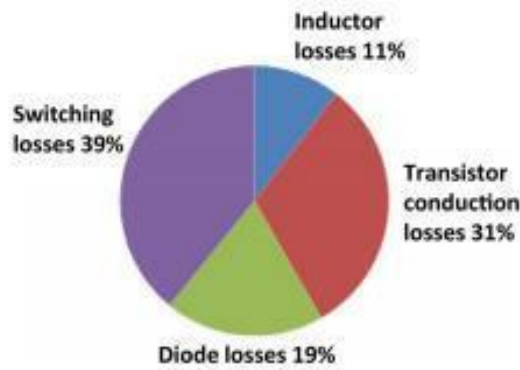


Figure 2.3.3: Power loss for dc-dc boost converter for GaN (approximate) [2]

## 2. 4: Efficiency for Converter

From a material point of view, both of the FETs have very similar parameters and characteristics but SiC performs better when the frequency is low and GaN can be used for high-frequency RF power applications [8].

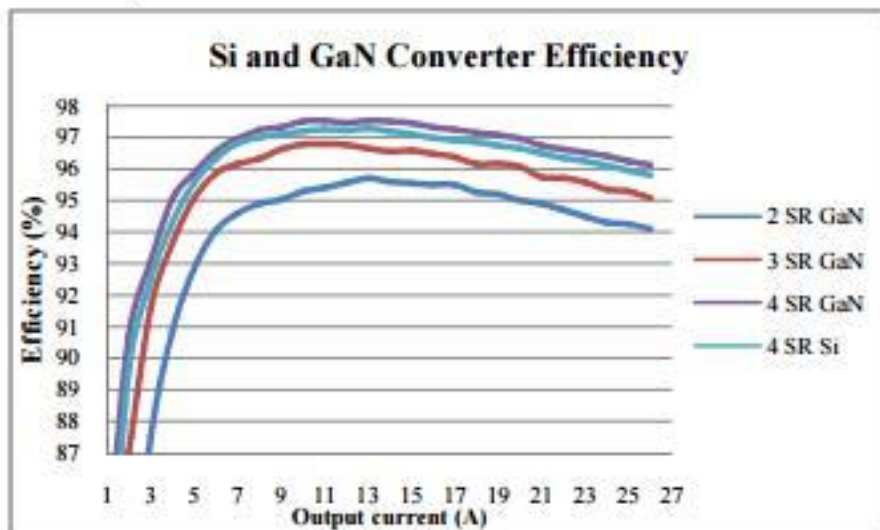


Figure 2.4.1: Efficiency comparison for Si-based and GaN converters

Figure 2.3.1 shows efficiency curves for two converters, with GaN, and with SiC. Another comparison for both GaN and Si-based with voltage ranging from 40 V-200 V is given below [15]. For soft-switching applications, losses related to switching are important and needed to be minimised by zero voltage and current switching. This represents efficiency and power loss for GaN and Si MOSFET. A comparison graph from [15] is shown below. When the switching frequency is 1.2 MHz the performance of both MOSFET is measured and plotted.

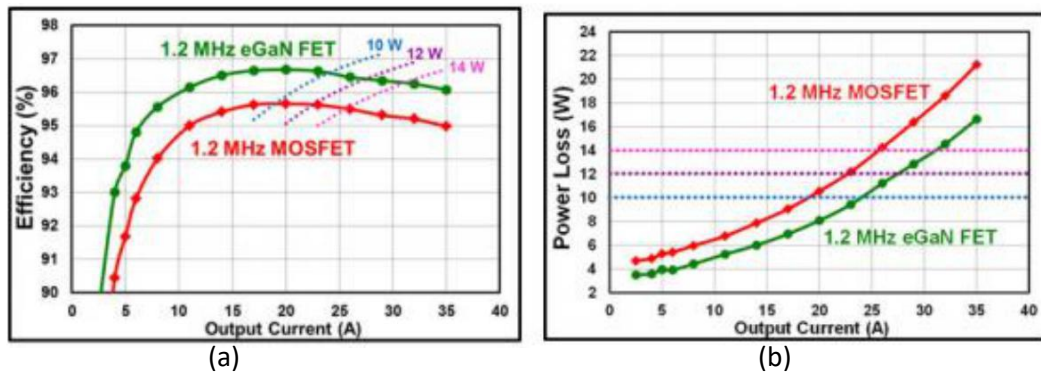


Figure 2.4.2: Efficiency (a) and power loss (b) comparison for GaN and Si MOSFETs [15]

Figure 2.3.2 (a) shows the efficiency percentage with respect to the output current. It is clear from the plotted graph the GaN has better efficiency than MOSFET when the operating frequency is 1.2 MHz. With the power loss at Figure 2.3.2 (b), at the same operating frequency, GaN has less power loss than MOSFET.

## 2.5 Material Properties

GaN has a high electron mobility because of the two-dimensional electron gas layer in between aluminum nitride layer and GaN layer. Thus, it can work for high-frequency applications. Due to the two-dimensional layer GaN HEMT has natural polarisation result at the junction and the polarisation in piezoelectric effect [16]. A schematic is shown below for the GaN HEMT.

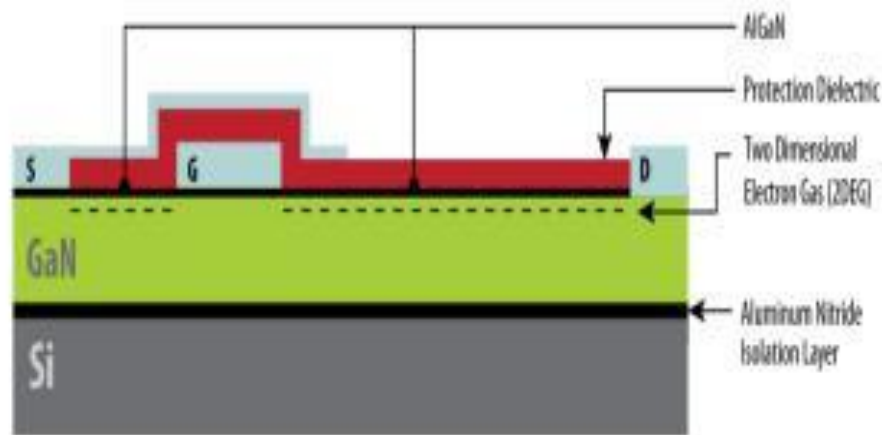


Figure 2.5.1: Cross Section of GaN [16]

GaN HEMT has current collapse phenomena and every GaN device has different phenomena characteristics to show. Up-to eighty-four percent efficiency has been achieved using GaN as switching device [2]. High electron mobility along with high saturation velocity for GaN and SiC allows these to operate in high frequency [8]. GaN also has properties of high thermal conductivity but SiC is found to have more thermal conductivity than GaN.



# Chapter 3

## Analysis for Simulation

### 3.1 Introduction to Basic Circuit

The task of converter electronic circuit is to convert one voltage level to another, the level of voltage may vary and it can be increased or decreased depending which type of converter circuit is used. This converter is widely used for battery operated devices but a major concern is an efficiency and size. Figure 3.1.1 shows the basic configuration of buck and boost converter circuit. A buck converter is used to lower voltage level and boost is to raise the level high.

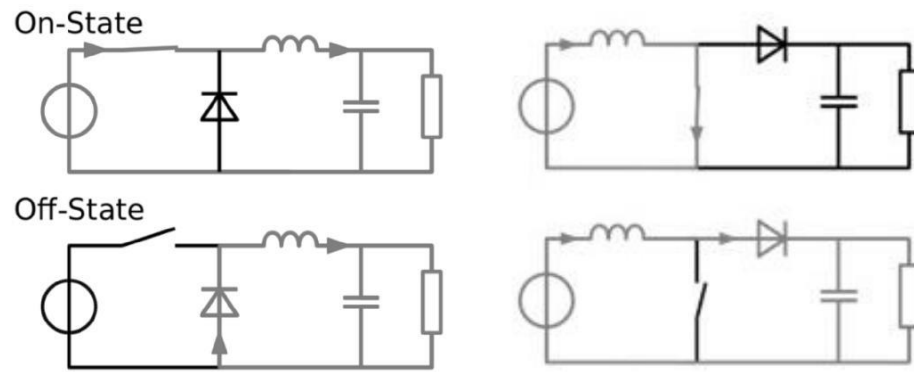


Figure 3.1.1: Buck (a) and Boost (b) converter on and off states

Converter plays a vital role when supplying energy to loads, not only for solar-powered appliances but also for use in other battery operated appliances like laptops, personal computers or Smart Phones or in a car.

A boost converter has two semiconductors, diode and transistor along with capacitor and inductor. The converter can have some voltage ripple and to reduce them, a filter is used. Capacitor and inductor works as storage element for a converter. The boost converter has two phases of work, switch closed and open operation. So during the closed switch cycle, the current will flow in clockwise direction through an inductor. Therefore the inductor will get to store some energy as there will be some magnetic field generated. And when the switch is open, the impedance will become higher. SO the amount of current will be less. The polarity for inductor will change to negative and this will cause a higher voltage to charge the capacitor. Depending on the switching cycle, inductor will not discharge when it is in charging stage. This will create a high voltage output in load side.

### 3.2: Simulation Circuit Diagram:

The test circuit used for GaN performance testing here is a boost converter. This will work to increasing the voltage from low to high. In this circuit three switching transistors are used to measure the output voltage level with different loads. The boost converter is a switch mode converter where the output voltage is higher than the input voltage. The fact for boost converter is,  $V_{IN} < V_{OUT}$ , and input current is higher than output current.

The required parameters were given so all the components were selected by calculation. The topology is the same as a basic boost converter. This will take a dc voltage as input and give a higher output voltage at the load side. The block diagram of the boost converter circuit is shown in figure 3.2.1

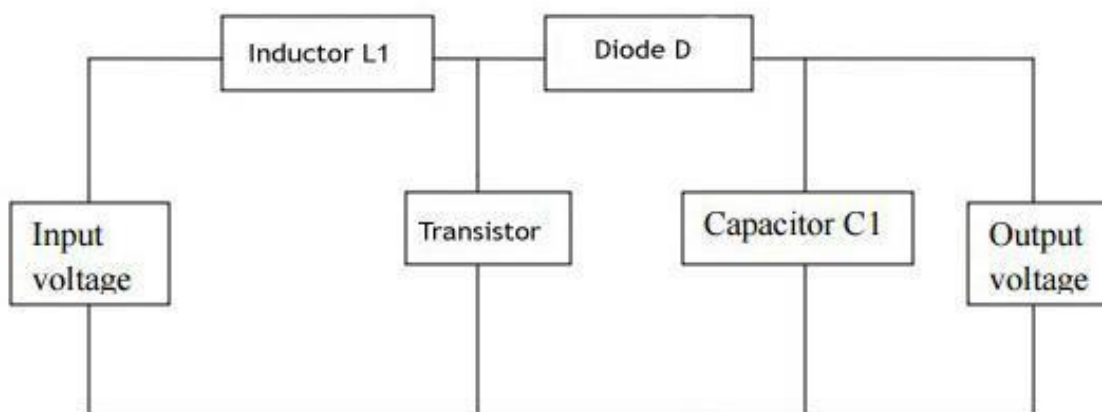


Figure 3.2.1: Block diagram of boost converter

An inductor, capacitor, and diode are used here along with the transistor. The task of the transistor is to work as a switch. The Input voltage is the supply voltage, which needs to be greater at the output. The voltage passes the current through the inductor making it store energy by creating a magnetic field.

The transistor is working here as a switch for the circuit. When the switch is on, diode will create an open circuit so at one side the voltage will be higher than other side. During close switching operation input voltage passes across the inductor and the diode will be open circuit. So the inductor will discharge through the diode, resistor and the capacitor. The switching transistor playing a vital role here because on it the efficiency of the overall converter depends. For switching on state, the period of time is found to be 5.5 ns and for switching-off state, 4.5 ns. All the components used for this boost converter circuit has been discussed later in this chapter.

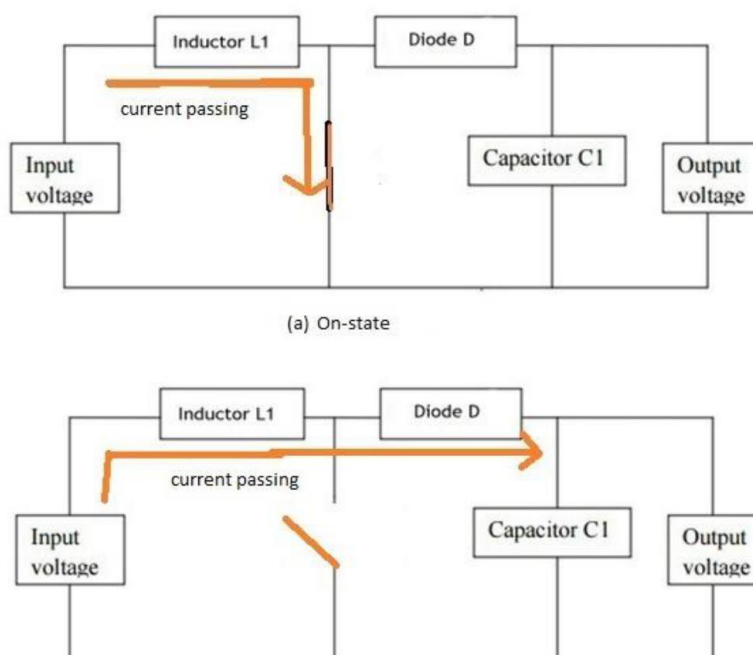


Figure 3.2.2 (a) On-state (b) Off-state operation of a boost converter

Solar power is mostly DC and thus if the load is also consuming DC power then we need a converter which can provide the required power at the load. Now consider a simple design topology for a load requirement as below, the input energy is coming from a solar source and is being stored in a battery, which supplies to the load as required. So the entire circuit will work following the flow chart at figure 3.2.3 [25].

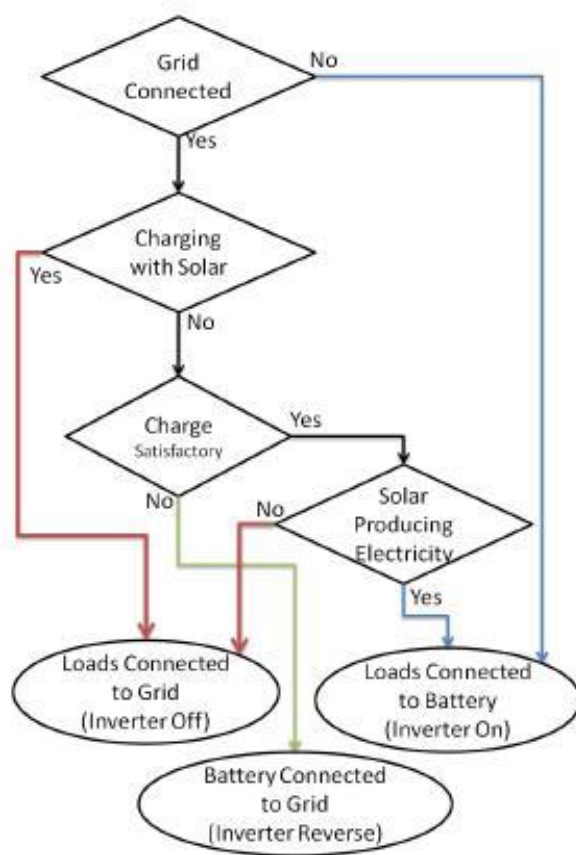


Figure 3.2.3: Flow chart of working principle for the solar power [25]

So the topology is made with the aim of charging the battery in two ways: when there is not enough solar energy to charge the battery, the system will connect to the grid for charging purposes. When there is enough solar power to charge the battery, it will supply the load if the charge stored is not enough to supply the load the batteries will be charged from the grid.

### 3.3 List of Requirements and Parameters:

Table 3.3.1: List of required parameters for design

Parameter	Corresponding values
Input voltage	5-5.5 V
Output voltage (expected)	12 V
Operating frequency	100 KHz

### 3.4 Design Calculation and Selection:

19

Now focus on the main point of this study of comparing the performance of switching devices for a DC-DC converter circuit.

#### 3.4.1 Duty Cycle Calculation:

The duty cycle is one of the most important for any boost converter circuit, because this finalizes the switching on and off states for the circuit so that the inductor can be charged. For the design here the calculations for the duty cycle as follows

$$\text{Duty Cycle, } D = 1 - \frac{V_{in} \times \eta}{V_{out}} \quad (3.1)$$

Here,  $V_{in}$  = Input Voltage for the circuit

$V_{out}$  = Desired Output Voltage  
= Efficiency (Approximately)

So, given the desired output and the given Input, we calculated the duty cycle, 0.61 for the circuit. We assume the converter circuit to be 85% efficient because on average almost all the converter circuits have this efficiency.

#### 3.4.2 Switching Frequency Selection:

To get high efficiency, the switching frequency is most important for a converter. The voltage across the inductor is also influenced by the switching frequency. The inductors of same structure gives a different value for different switching frequency, also electric current at maximum efficiency differs. For higher switching frequency, FET and IC's charge-discharge quiescent current also increases.

Table3.4.2: Switching frequency effect on properties

Properties	Low	High
Maximum efficiency	High	Low
Output current at max efficiency	Light Load	Heavy Load
Ripple	Large	Small
Response	Slow	Fast

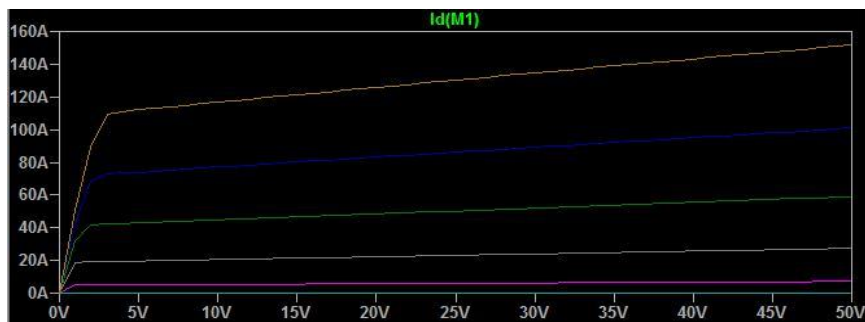
### 3.4.3 Transistor Selection:

The main purpose of this study was to compare different transistors to see which has better performance in terms of load. So three different transistors were used as the switching FET and their output was measured to compare them. These transistors were chosen as they have very similar parameters so should perform similarly. Thus it will be easier to make a decision from the output which FET actually performs well with given requirements.

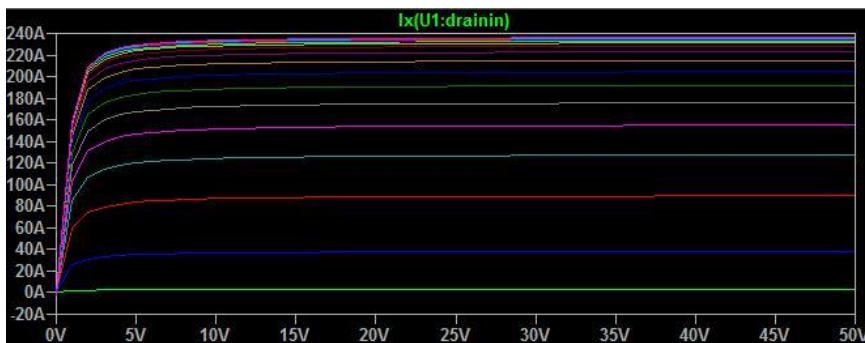
Table 3.4.3.1: Switching transistor name and model number

Name of the IC	Type	Manufacturer
FDB2532	N Channel MOSFET	Farichild
EPC2001	GaN	EPC Corp.
C2M0025120D	SiC	Cree Inc.

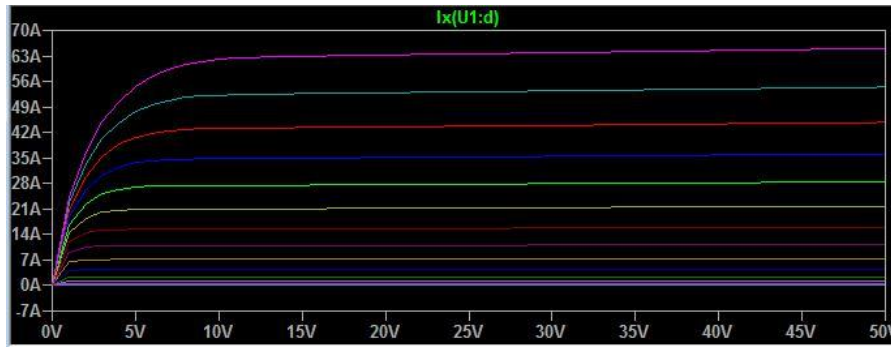
I-V characteristics for three transistors are shown in Figure 3.3.1



a) Simulated  $I_D$  vs  $V_{GS}$  for FDB2532



b) Simulated  $I_D$  vs  $V_{GS}$  for EPC2001



c) Simulated  $I_D$  vs  $V_{GS}$  for C2M0025120D

Figure 3.4.3.1: I-V Characteristics Curve for three transistors

In figure 3.4.3.1 the curves were plotted with respect to drain current as a function of voltage from drain to source. The dc voltage sweep for the input varied from 2V to 10V with 0.5 increments to check the drain current. On the Y axis drain current ( $I_D$ ) and on the X axis gate to source voltage ( $V_{GS}$ ) was plotted.

To get the best results the transistor needs to be selected for the maximum voltage and current ratings. Switching losses occurs especially for and, but these oppose each other. For smaller  $R_{DS}$  and  $C_{ISS}$  the total performance loss is also smaller. The transistors model used here for the simulations circuit, has below mentioned parameters,

Table 3.4.3.2: Transistor parameters as per data sheet

Transistor	$V_{DSS}$ (V)	$V_{GS}$ (V)	$I_D$ (A)	$R_{DS}$ ( $\Omega$ )	$V_{GS(TH)}$ (V)
<b>FDB2532</b>	150	$\pm 20V$	79	0.014~ 0.048	2~ 4
<b>EPC2001</b>	100	$\pm 20V$	25	0.0056~ 0.007	0.7~ 2.5
<b>C2M0025120D</b>	1200	-10/ +25	90	0.034	2~ 4

#### 3.4.4 Inductor Selection ( $L_1$ ):

For better efficiency, it is required to have small coil losses and to minimise the loss inductor needs to have small  $R_{DC}$  value. If the inductor value is too large then the  $R_{DC}$  value increases, which effects on efficiency and makes it low during high load periods. The higher inductor value can lead to higher output current as it can reduce the output ripple current. The efficiency and dimensions can determine the perfect inductor value. The inductor value can be calculated with respect to time variation equation. But mostly the value is selected with configuration of the converter circuit. So the equation for inductor value can be measure by,

$$L = V_L \frac{dt}{di} \quad (3.2)$$

where

$L$  = Inductor value

$V_L$  = Maximum voltage across the inductor

### 3.4.5 Diode Selection ( $D_1$ ):

The losses caused by the diodes are actually the sum of the heat loss and losses due to reverse leakage current. Therefore it is important to choose similar values of loss from both forward biased voltage and leakage current. Typically the Schottky Barrier Diode (SBD) have characteristics of creating less loss. The SBD selected here is MBR140, which has forward current ratings of 1A, and forward voltage 600mV at ambient temperature upto 120 °C. This SBD gives power dissipation of 0.6 W, which is very low and the forward current is according to expected maximum output current.

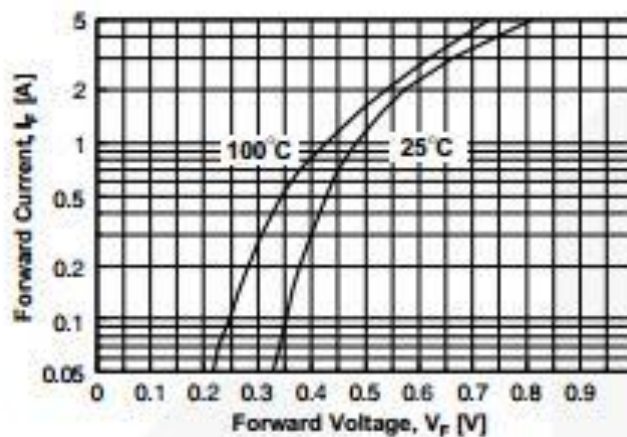


Figure 3.4.5.1: Forward voltage characteristics for diode [71]

Any SBD that has large forward voltage but a small leakage current shows excellent properties for a light load but it has some drawbacks in heavy loads. MBR140 is a Schottky Rectifier manufactured by Fairchild Semiconductor Corporation.

### 3.4.6: Capacitance selection:

The capacitor plays an important role in making the output ripple smaller, and large value to reduce the ripple. But an unnecessary large value of the capacitance might lead to a cost increment as well. So it is really important to choose a capacitance value to suit the ripple level targeted. Another important characteristic of a capacitor is what material it is made of, and the capacitor used for the circuit is type X5R and has low equivalent series resistor value. This is a ceramic capacitor with a value of 10  $\mu$ F. The capacitor selection for boost converter circuit is also depends on the output



maximum current level. The value 10 uF for output capacitor used here from the range of capacitor to be used for the circuit calculations. The equation we can use here for selecting the range of capacitor is given below,

$$C = \frac{I_{out(max)} \times D}{Frequency \times \Delta V_{out}} \quad (3.3)$$

Here,

$I_{out(max)}$  = Maximum output current desired

$\Delta V_{out}$  = Maximum output voltage ripple

# Chapter 4

## Circuit Description and Simulation

A very basic boost converter circuit is used here to run the simulations and test the circuit. This was to measure the performance of the switching transistors and compare their output voltage. The basic topology of boost converter used here has a transistor as a switch and this was given a pulse to turn it on and off. During the on- mode of the transistor, the current was passing through the inductor to get energy, and through the diode, it was passed to the capacitor for storing. And at off-state, this will become a short circuit as described in Chapter 3. Therefore, the voltage we are measuring through the load is actually the stored capacitor voltage.

#### 4.1: Requirements for the design:

Table 4.1.1: Component parameters for the design

Component	Requirements
Switching frequency	100 KHz
Input Voltage	5 V-5.5 V
Desired Voltage Output	12 V
Ripple current	100 mA (max)
Efficiency	85% assumed

#### 4.2: Calculations and Circuit Diagram:

The required components were calculated based on the design requirements. To calculate the duty cycle (3.2) was being used from Chapter 3. So the Average Duty cycle is found to be 0.61, which is quite normal for the boost converter. To choose the inductor value from the switching transistors data sheet, the value is chosen to be approximate 298  $\mu\text{H}$ .

This value of inductor will be used for three of the switching transistors to compare the performance. For the capacitor value selections, it was designed according to the switching frequency and thereby kept within the 10  $\mu\text{F}$  range as described before in Chapter 3. All the transistor models used for this simulation are practical LTSpice model provided by their manufacturer. The Period of time for the gate turn-on voltage used here according to the duty cycle calculations, it has been used for 10 $\mu\text{s}$  to keep it within the duty cycle value 0.61.

##### 4.2.1 Converter with NMOS:

The first circuit is shown in Figure 4.2.1 with the transistor FDB2532 as the switch, an N-Channel MOSFET in enhancement mode which has ratings of 150 V, 79 A and 16 m $\Omega$ . This transistor has low Miller charge and is suitable for synchronous rectifiers.

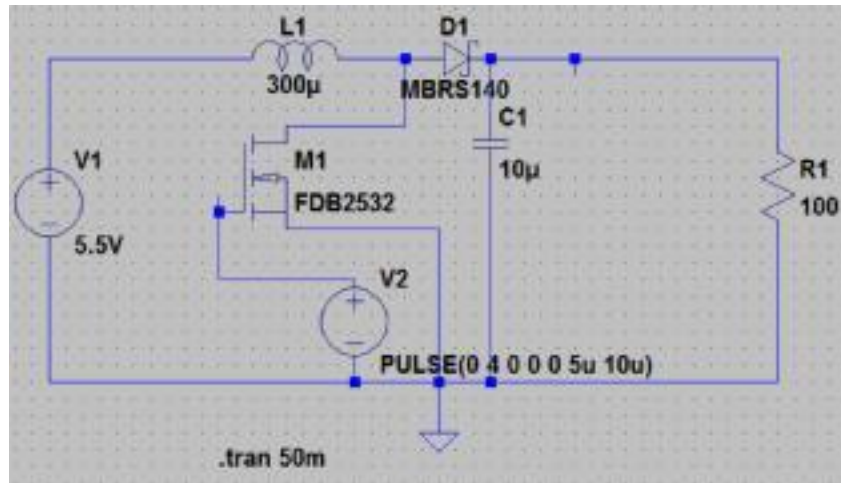


Figure 4.2.1 Converter with FDB2532

The source V2 is the positive gate turn-on voltage for the transistor to turn it on to function as a switch. The pulse provided here,

Table 4.2.1.1 FDB2532 supply voltage

Component	Ratings
Gate turn on voltage	4 V
Ton	5 $\mu$ s
Tperiod	10 $\mu$ s

The turn-on voltage used here is the minimum voltage to turn this switch on as per given in the datasheet, less than this voltage this switch is not on.

#### 4.2.2: Converter with GaN

The other transistor used for GaN is an EPC2001 model which has ratings of 100 V, 25 A, and 7 m $\Omega$ . This is grown on a silicon wafer and has high electron mobility with a low-temperature coefficient [9]. This enhancement-mode power transistor is able to do high-frequency switching and at the same time has low on-state losses. The circuit diagram is showed here in figure,

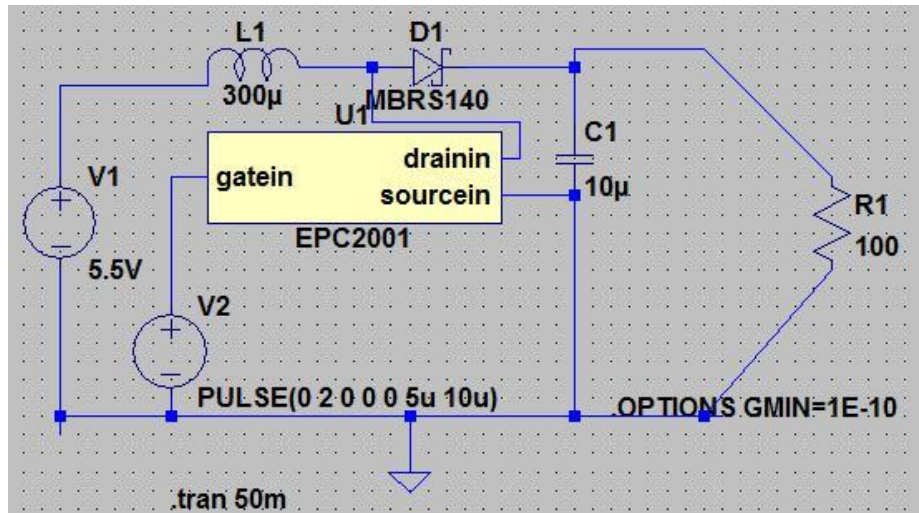


Figure 4.2.2: Converter with EPC2001

The gate turn-on voltage provided for EPC2001 is given below,

Table 4.2.2 EPC2001 supply voltage

Component	Ratings
Gate turn on voltage	3 V
Ton	5 $\mu$ s
Tperiod	10 $\mu$ s

The turn-on voltage used here is 3 V. A GaN transistor needs even less than this voltage to turn it on. The circuit was tested with 2 V supply voltage and yet this switch was giving better output voltage, this effect of gate turn-on voltage is discussed in Chapter 5 with simulated results.

#### 4.2.3 Converter with SiC

The SiC switching transistor used here is from CREE Inc, and the model is C2M0025120D. The circuit diagram drawn in LTSpice is given below. This transistor has ratings as per data sheet of 1200 V, 90 A with drain- source on- state resistor of 34m $\Omega$ . This is N-Channel enhancement mode silicon carbide power MOSFET. This is mostly used for high voltage dc-dc converters but as this model is commercially available from the manufacturer, this is being used to test the performance with a GaN.

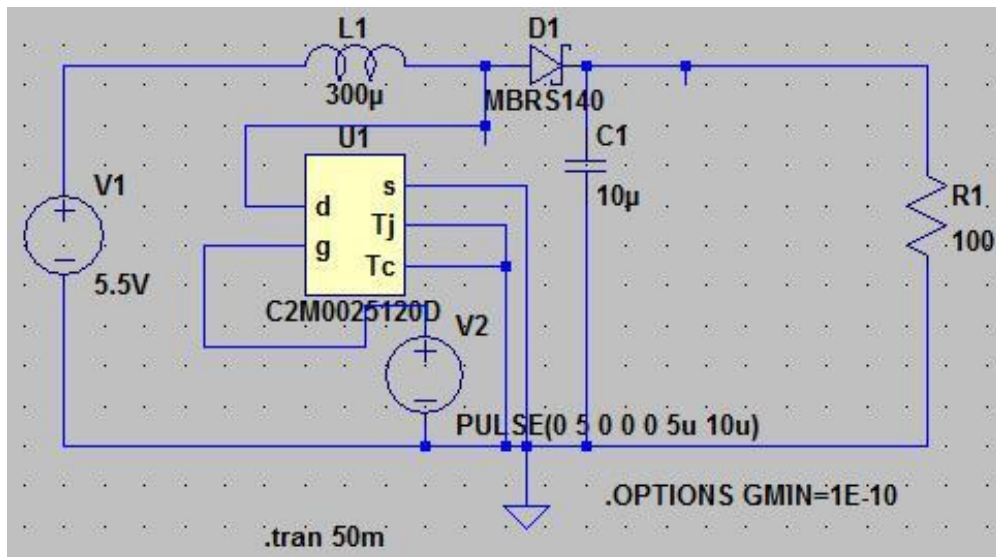


Figure 4.2.3: Converter circuit with C2M0025120D

The gate

Table 4.2.3 C2M0025120D supply voltage

Component	Ratings
Gate turn on voltage	5V
Ton	5us
Tperiod	10us

### 4.3: Output Graph of Different Transistors

A common problem of the boost converter circuit is output ripples at a high frequency. Therefore when the circuit was simulated in LTSPice, the inductor and the capacitor value were chosen carefully as described in Chapter 3, so that we can avoid the voltage ripple. The combination of inductor and capacitor value also filtered the output ripples. With a varying load, the output was recorded for all three transistors. And an output graph across to the load for the boost converter circuit simulated here, was taken into consideration for the final outcome of the study.

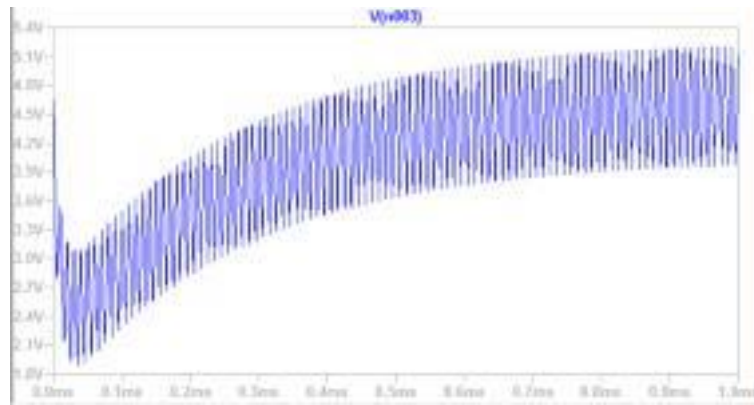


Figure 4.3.1: Simulated output voltage with 1  $\Omega$  load with FDB2532

When the load of the converter is 1 $\Omega$  with an FDB2532 switching transistor, the output graph is plotted in Figure 4.3.1, it shows the output is less than to the input voltage. At this point the efficiency of the converter is calculated very low, 0.54. The simulation was run only for 1 ms as this has got some ripples at the output voltage.

Now we have simulated the same circuit with EPC2001 as a switch, and below Figure 4.3.2 were found.

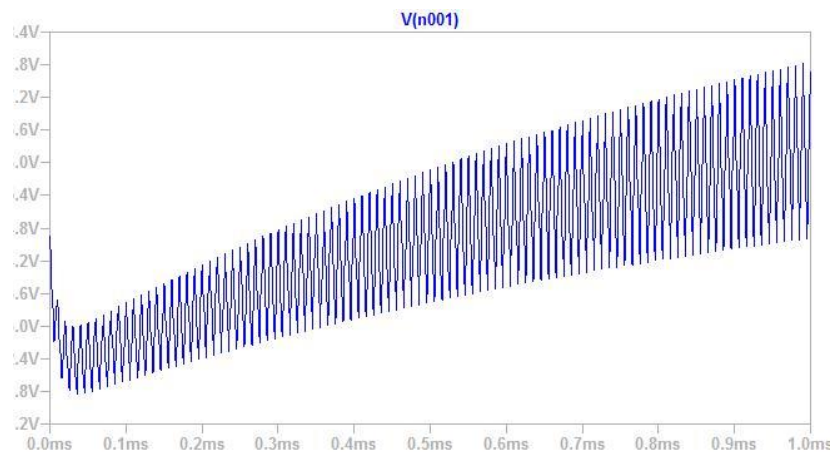


Figure 4.3.2: Simulated output voltage with 1  $\Omega$  load with EPC2001

So when we tested the same circuit using GaN transistor EPC2001 with the same load but even smaller gate turn-on pulse voltage of 3 V the output was better than for the NMOS transistor. It is clearly shown from the plotted output that this converter operating in same frequency giving an average value of 8.75V. The efficiency calculated was 0.75 across this load. This output voltage has got lots of ripples as well like the FDB2532 but this has converted the output voltage to a higher level than the input voltage.

Now with the same parameters, this circuit was developed with SiC transistor, C2M0025120D and the output were plotted.

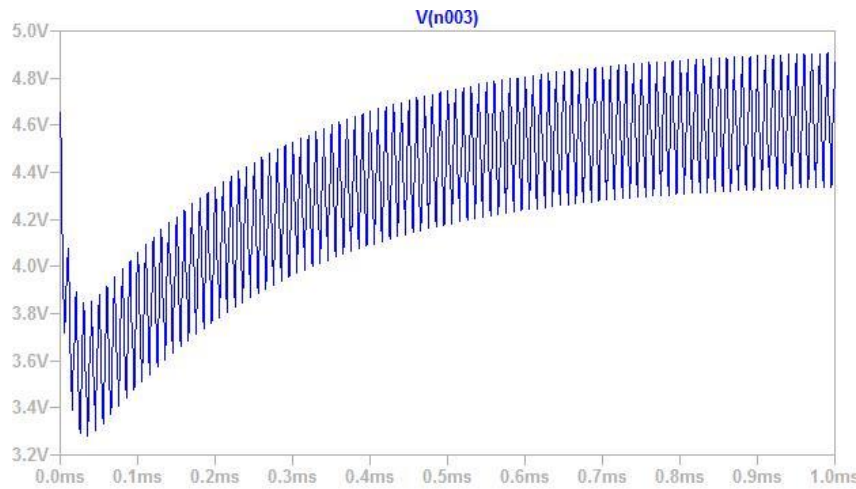


Figure 4.3.3: Simulated output voltage at 1  $\Omega$  load with C2M0025120D

The output shows an average of 4.65V across the load and the efficiency found for this is 0.67 when it has a load of 1  $\Omega$ . Which means that this converter circuit with a SiC transistor is unable to give good efficiency. The SiC transistor and the NMOS transistor has same output and same ripple at the output.

To recheck the output value with the three different transistors the boost converter circuit was tested with a load 20  $\Omega$ . As has been mentioned, for three transistors the output will be recorded across the loads by varying. Along with voltage, the input current and output current were also measured and thus the efficiency calculated for that particular load.

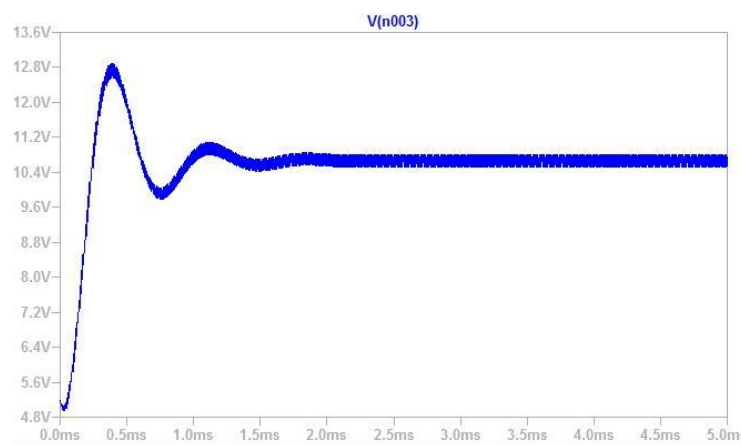


Figure 4.3.4: Simulated output voltage with load 20  $\Omega$  for FDB2532



The output graph for a  $20\ \Omega$  load shows an average output of 10.65 V. The efficiency calculated at this load is 0.92. When the load was  $20\ \Omega$ , the output ripple has reduced a lot compare to  $1\ \Omega$  load for the same transistor.

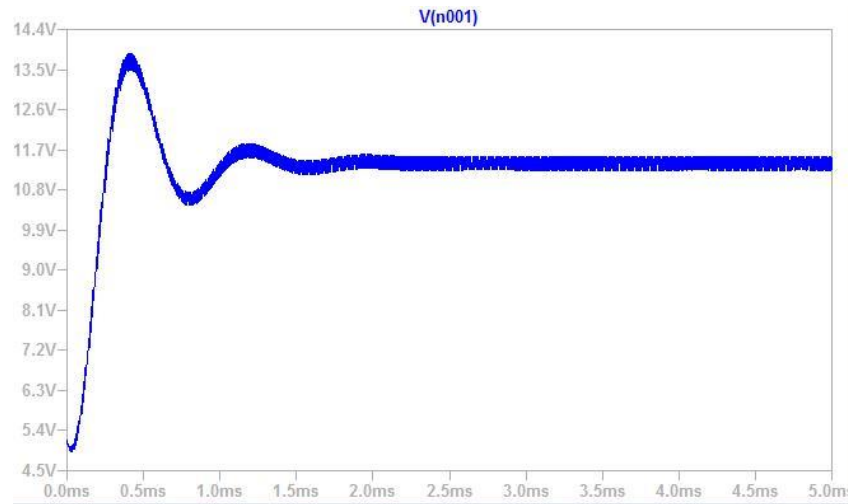


Figure: 4.3.5: Simulated output voltage with load  $20\ \Omega$  for EPC2001

Output voltage at Figure 4.3.5 shows an average voltage of 11.4 V with an EPC2001 transistor as a switch with a  $20\text{-}\Omega$  load. The efficiency at this point is 0.94 which is already higher than with FDB2532 transistor. The ripple at the output voltage has been reduced compare to  $1\ \Omega$  load for EPC2001 transistor.

We tested the circuit with a SiC transistor and the output is shown below.

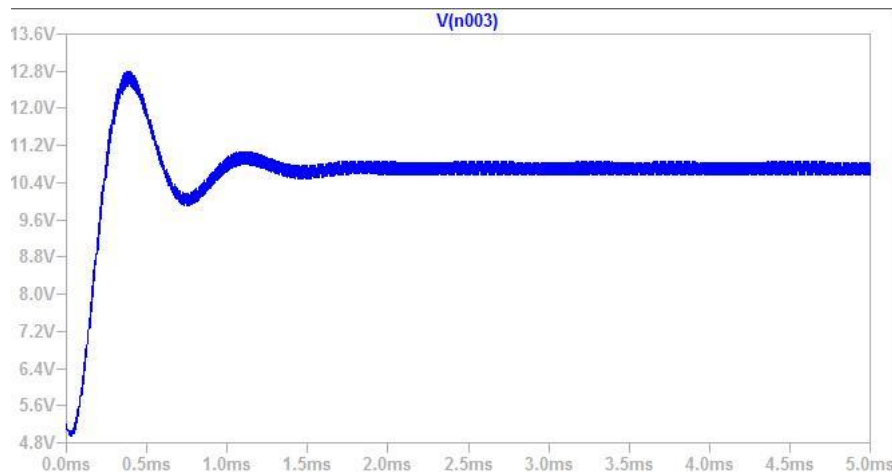


Figure 4.3.6: Simulated output voltage with load  $20\ \Omega$  for C2M0025120D

The SiC transistor, C2M0025120D, gives an output of 10.7 V with an efficiency of 0.92, which is equal with an NMOS transistor and shows that the EPC2001 gives better output and efficiency. And small ripple at output has been observed for this transistor.

When recording the output voltage with various load, an optimum load point was discovered for each transistor [Table 5.1]. So now we have taken measurements of that optimum load-point efficiency for each transistor to compare their efficiencies. Therefore the 70  $\Omega$  load point is selected, as at this point GaN and SiC have started showing the optimum voltage point. So choosing this load value for the output to compare how the converter actually performs will be best idea to get a clear view of the efficiency for each transistor.

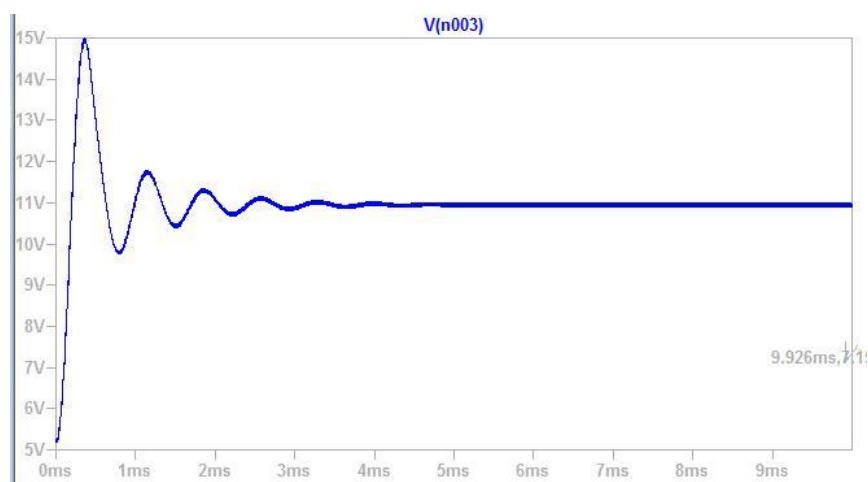


Figure 4.3.7: Simulated output voltage with 70  $\Omega$  load for FDB2532

As described the load of 70  $\Omega$ , the voltage output for FDB2532 has 10.95V with an efficiency factor of 0.94. Now comparing to previous graph for the same transistor, ripple has clearly be found to be less and almost a steady line has found as dc output.

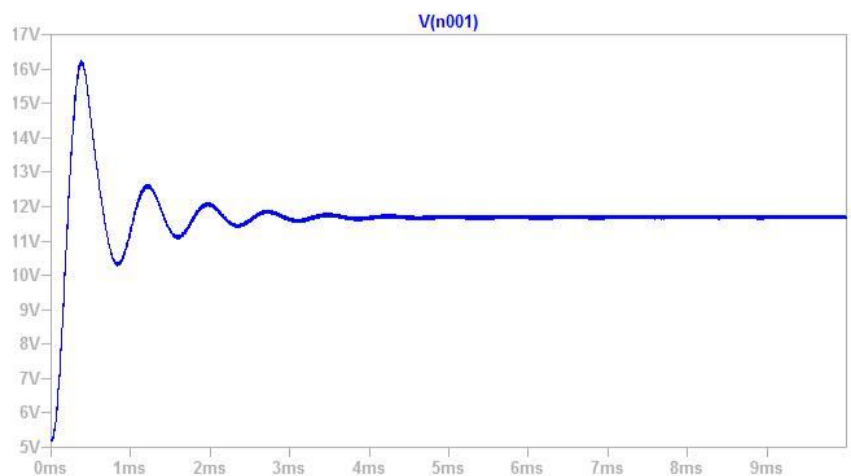


Figure 4.3.8: Simulated output voltage with 70  $\Omega$  load for EPC2001

The EPC2001 has an output voltage of 11.68 V with a 70  $\Omega$  load and the efficiency is 0.99, so it has maximum efficiency at this point with the given operating frequency. The output ripple has almost found to be less than of load 20  $\Omega$  for the same transistor. Now the output for the C2M0025120D has to be checked and the simulation result is showed in the next figure.

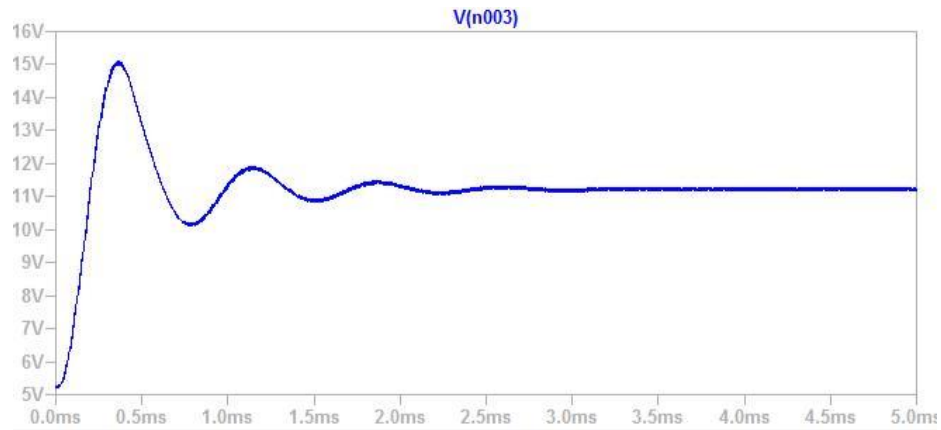


Figure 4.3.9: Simulated output voltage with 70  $\Omega$  load for C2M0025120D

The C2M0025120D has an output voltage of 11.22 V with efficiency of 0.94. At this simulated output it has been clearly seen the output ripple has reduced a lot and it is almost getting a steady state line.

Now the load was taken to 100  $\Omega$  to check how the circuit would behave for higher loads even after getting the voltage output cut-off point.

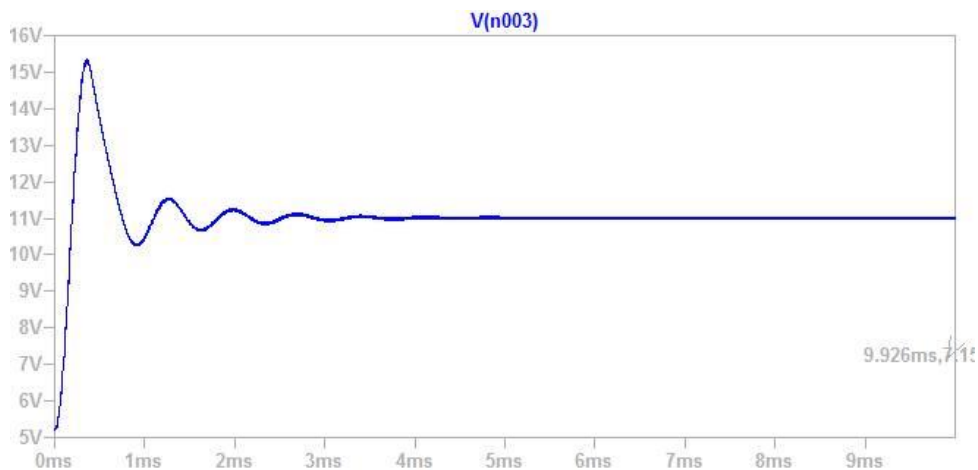


Figure 4.3.10: FDB2532 Output for 100  $\Omega$

With a 100  $\Omega$  load FDB2532 has 11V at output with efficiency of 0.94. The ripple is not visible at this load.

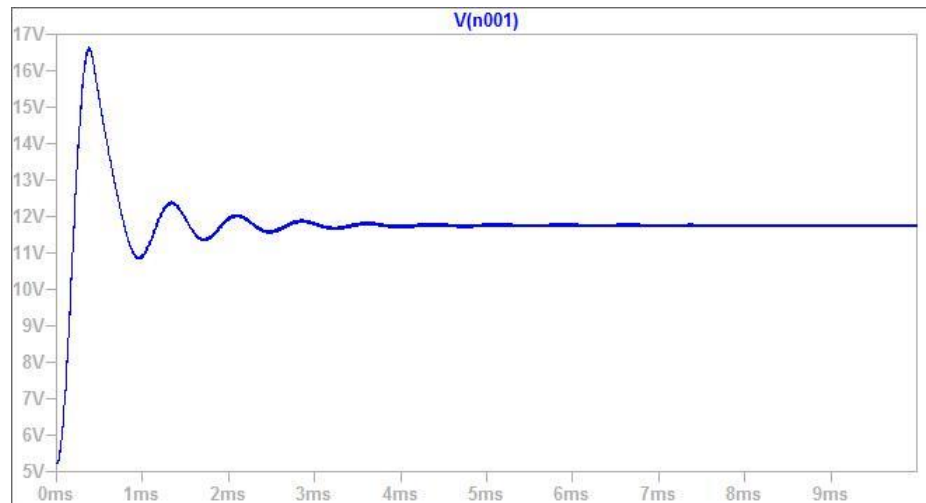


Figure 4.3.11: EPC2001 output with 100  $\Omega$  load

The input current is to be found 260 mA with output voltage of 11.75 V for EPC2001. The calculated efficiency is 0.97 which is near to its highest efficiency, for a load of 70  $\Omega$ .

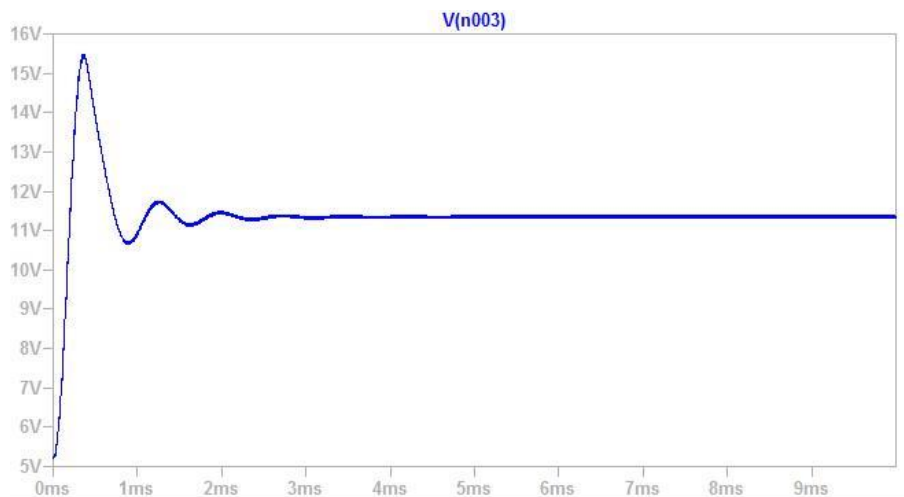


Figure 4.3.12: C2M0025120D output for 100  $\Omega$  load

The SiC transistor gives an output voltage of 11.35 V with an efficiency of 0.93 and input current of 0.25 A. So even having the same material properties, with the given frequency of 100 kHz, SiC transistor is unable to provide efficiency even equal to GaN transistor.

The complete set of data found in this simulation is provided in next chapter. Also, comparison graphs for the three transistors are shown. These graphs will lead us to take a final decision of which transistor gives better performance for switching. But from the measured figures of output voltages, it is clear that GaN can give higher efficiency than two other transistors.

# Chapter 5

## Outcome and Results

In this chapter, the outputs found from the simulation of LTSpice will be discussed. As we have simulated a boost converter circuit with three different transistors to see which transistor has a better efficiency, the efficiency was calculated from output power and input power. The output power and the input power were measured as per below mentioned equations,

$$P_{out} = V_{out} \times I_{out} \quad (5.1)$$

$$P_{in} = V_{in} \times I_{in} \quad (5.2)$$

The results found from the output for different loads for three transistors are shown below in table 5.1.1. The load was from 1  $\Omega$  to 100  $\Omega$  to check the output voltage graph and see where the optimum output voltage point can be found.

### 5.1: Output Voltage With Respect to Load:

Table 5.1.1: Output voltage measured with respect to different load

Load ( $\Omega$ )	FDB2532 (V)	EPC2001 (V)	C2M0025120D (V)
1	4.7	8.8	4.65
10	10.3	11.1	9.95
20	10.7	11.4	10.7
30	10.8	11.5	10.9
40	10.8	11.6	11.02
50	10.9	11.6	11.1
60	11	11.6	11.2
70	11	11.7	11.2
80	11	11.7	11.2
90	11	11.7	11.3
100	11	11.7	11.3

This table indicates that the EPC2001 provides the highest output for this simulated boost converter. Also, a comparison graph has been plotted as well to show how the output voltage is actually differing for the different transistor.

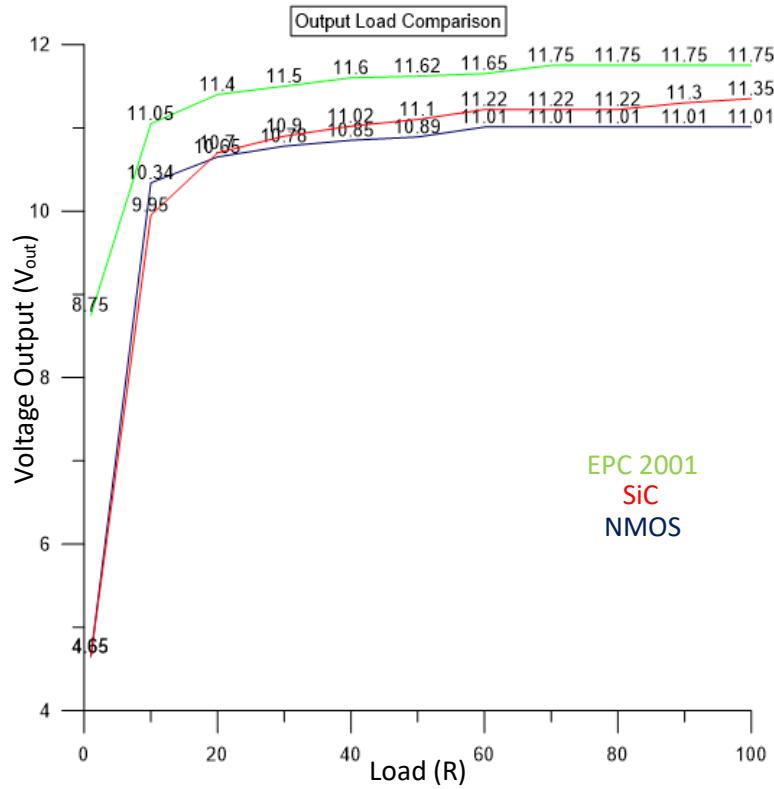


Figure 5.1.1: Output voltage comparison for three transistors

This figure shows the output voltage measured with various loads. The loads are presented at X axis and measured output voltages at the Y axis. The comparison graph of different transistors shows that EPC 2001, the GaN transistor can give a high output voltage with small load compare to NMOS transistor and the SiC transistor. When the load is 60  $\Omega$ , the output has already started reaching the steady- state point for the FDB2532. At a 70  $\Omega$  load for EPC2001, the output is found to be a maximum and the efficiency is 0.97. But when we look into the low load point of these transistors, we can see that EPC2001 has proven capability of delivering a high output voltage, which means GaN transistor is actually able to take the low load and can give a high voltage output.

## 5.2: Efficiency with Load:

The efficiency calculations of the three transistors were also done as follows,

$$\eta = \frac{V_{out} \times I_{out}}{V_{in} \times I_{in}} \quad (5.3)$$

Where,

$V_{\text{out}}$  = Output Voltage

$I_{\text{out}}$  = Output Current

$V_{\text{in}}$  = Input Voltage

$I_{\text{in}}$  = Input Current

As this is dc-dc converter and the output has oscillations, the average voltage and current were measured and calculated from the simulation for output to calculate the power.

Table 5.2.1 lists the differences in efficiency for three transistors

Table 5.2.1: Efficiency for Transistors

<b>R (<math>\Omega</math>)</b>	<b>FDB2532</b>	<b>EPC2001</b>	<b>C2M0025120D</b>
1	0.55	0.75	0.67
10	0.91	0.93	0.88
20	0.92	0.95	0.93
30	0.94	0.95	0.94
40	0.94	0.95	0.94
50	0.95	0.95	0.94
60	0.95	0.96	0.95
70	0.95	0.98	0.95
80	0.95	0.97	0.95
90	0.98	0.99	0.94
100	0.96	0.97	0.93

Now from the table of efficiency we can easily see that the EPC2001 has better efficiency for heavy load and for the lighter load it can deliver better voltage output but the efficiency is decreased. But the FDB2532 has given very poor efficiency with light load and for higher load the FDB2532 is not able to provide output voltage more than 11V where EPC2001 can give much better output voltage which is 11.8 V. The optimum voltage output for the FDB2532 and the C2M0025120D are 11 V and 11.3 V where the GaN transistor, EPC2001 has voltage output of 11.8V, this means that



the GaN transistor is able to handle much higher load compare to the NMOS and the SiC transistors. The efficiency comparison graph is shown below.

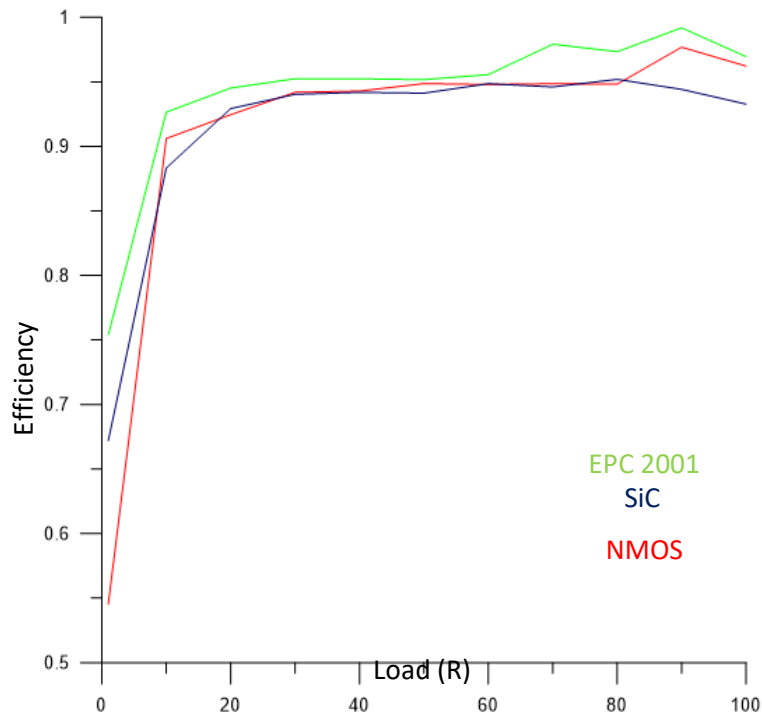


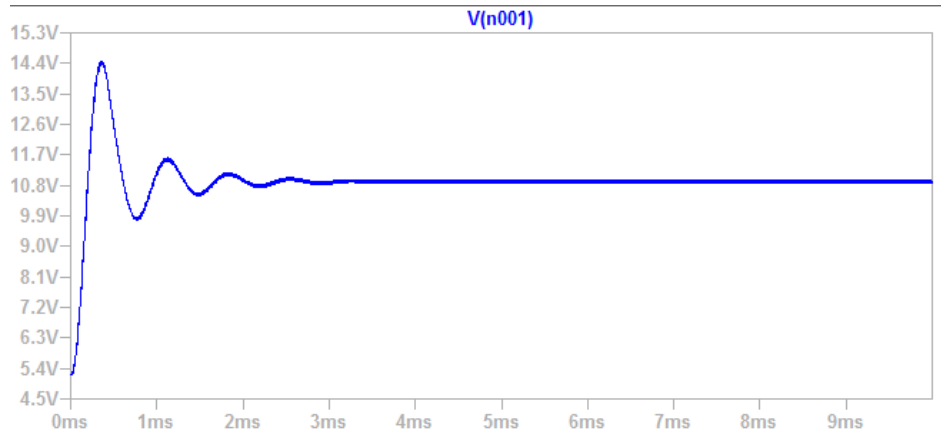
Figure 5.2.1: Efficiency comparison of three Transistors

### 5.3: Transistor Switching Turn-on Gate Voltage:

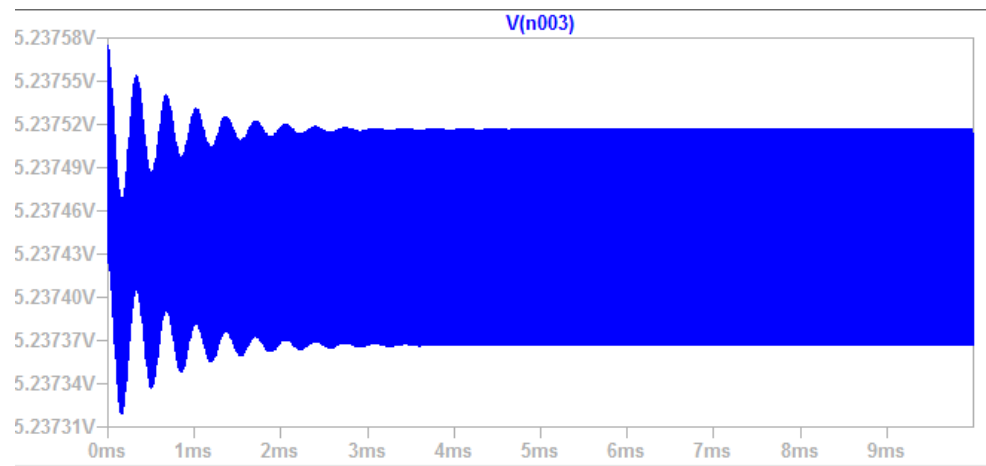
Another crucial point to discuss here is the turn-on voltage pint for these transistors. It already has been mentioned at Chapter 3 that the gate turn-on voltage for the EPC2001 was 3V and the FDB2532 is 4V. The FDB2532 was working with any gate turn-on voltage less than that voltage, which shows that the EPC2001 is taking low gate on voltage to turn on. This will actually decrease the power consumption and increase the battery life for battery operated devices like mobile, laptops or cars. As battery operated devices always has an issue with battery life, the EPC2001 is very good options to be used in such devices.

The wide band gap semiconductor like GaN has the capacity of fast switching with low switching loss. The power dissipation for EPC2001 is only 4.044  $\mu\text{W}$ , this can be found from thr released model data of EPC2001. This is very much beneficial for high power efficiency.

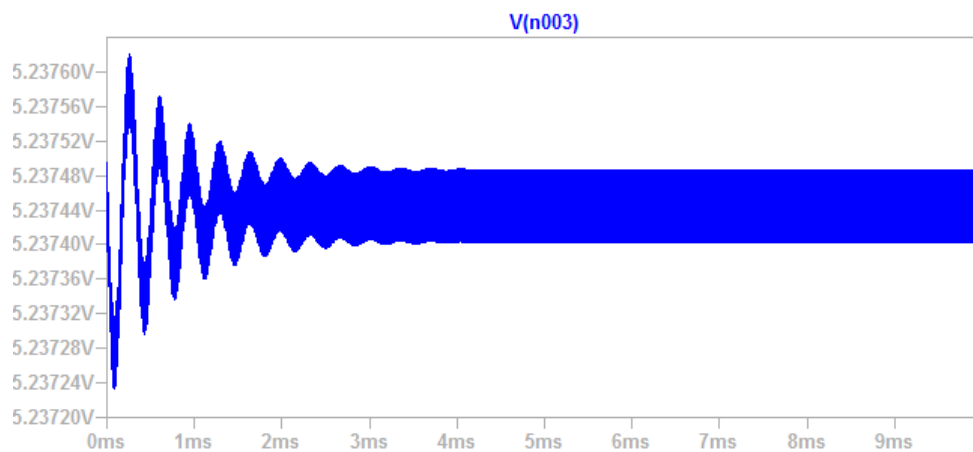
Figure 5.3.1 shows the output graph of three different transistors, when the gate turn-on voltage is set to 2V.



(a) EPC2001 with 70- $\Omega$  load and 2V gate turn-on voltage



(b) FDB2532 with 70- $\Omega$  load and 2V gate turn-on voltage



(c) C2M0025120D with 70- $\Omega$  load and 2V gate turn-on voltage

Figure 5.3.1: Gate turn-on pulse voltage comparison

From Figure 5.3.1 it can be clearly seen that the FDB2532 and C2M0025120D are not even turned on when the gate voltage is 2V, but EPC2001 is already on and giving an output voltage of approximate 10.90 V. The only visible output for NMOS and SIC transistor is oscillations. It has been

checked with the simulator that even with gate voltage of 3V the FDB2532 and the C2M0025120D are not working as switch and require a much higher voltage 4 V for FDB2532 and 5 V at least to turn it on. So a conclusion can be drawn from this is GaN requires less voltage for turn-on and give much higher efficiency than NMOS and SiC transistors in dc-dc conversion.

#### **5.4 Comparision between GaN and SiC:**

For comparing the performance in RF and power switching with another wide band gap material, Silicon Carbide transistor C2M0025120D was chosen from the Cree Company. A summary of material properties was shown for GaN and SiC in chapter 2. In the field of power applications, GaN and SiC plays an almost equal role but depending on conditions GaN performs better. From this simulation, it has been found that the performance of GaN is much better than SiC. From the efficiency chart given in Table 5.2.1, it has been shown that, despite having same materialistic properties GaN gives much better efficiency. Here the NMOS transistor is not coming into the comparison as it has different materialistic properties and is not a wide band gap semiconductor.

# Chapter 6

## Conclusion

As a wide-band gap semiconductor material, GaN has become a prominent and heavily used semiconductor material. The EPC2001 is a GaN transistor from EPC Corp that is commercially available and ready to use, though a newer version has been released recently. This study makes a performance comparison of three different transistors, in two different material. The simulations outcome, it has been clear that GaN gives better performance although the operating parameter of this transistor is lower than other two transistors. Three points can be discussed from this simulation, one is voltage output across the load, second is the efficiency factor and the third is a turn on gate voltage for the transistor.

## 6.1: Summary of Study

From the first point of view, the output voltage of a boost converter circuit using a GaN as switching device is much better than NMOS and SiC, even though SiC is supposed to have nearby output or better output compare to GaN. The SiC and GaN have same materialistic properties of giving the same output.

The second point is the efficiency of the converter. The circuit components were calculated with the assumption of being 85% efficient but this circuit has given above 90% efficiency. But this is not a real-time simulation, just software-based simulations. So the actual efficiency of a practical circuit may be different. Yet it is to be assumed that, it will not go below 85%. When we have compared three transistors, GaN transistor is again better than the other two transistors. It has given higher efficiency for all loads. For any converter, efficiency is very important as it is a boost converter, and for shifting the voltage higher from the input must have better efficiency. Typically the boost converters expected to have 80% efficiency.

The third and last point is the switching gate-on voltage. The GaN transistor was able to give output even at a very low switching pulse voltage. This is very important when it comes to battery-operated appliances like a cell phone or laptop or car. Battery life is very crucial point these days. If the circuit is required to provide more pulse voltage then the battery life will decay very fast and, from a user point of view, this is disappointing. Since GaN requires a very low pulse voltage, the battery life can stay longer than with other transistors.

## 6.2: Scope of future work


RF device technology is not only important for regular use, but also in the military market it has a vital use for legacy technology. For use in aviation or radar technology or in telecommunications, the development of RF technology is required. Thus, the development of power amplifiers is proceeding day by day. The material LDMOS is used usually at a frequency of 3 GHz for wireless applications. Though the GaN transistors has mechanical stability compare to LDMOS and also better heat capacity, therefore the prospect to be used in the military application is wide for the GaN.

The comparison of performance for GaN is done in this study for a boost converter. There is scope for work with GaN for a SEPIC converter as well. In the SEPIC converter, circuit optimisation is also possible and in future, there is a scope of work in that field. Also, there is the scope of built the circuit in practical at the lab and test all the data fund through simulations and check how

similarities they have. GaN is popular for use in the low-power high-frequency area and SiC seems suited to the high power, high voltage application area. In terms of cost efficiency, for both of the material, if silicon substrate is used, the cost for GaN will decrease a lot. For power application area GaN is getting more attention if high power is not required and the cost is a major concern [8]. The converters have always been appreciated in solar energy systems. In this study a basic boost converter circuit performance has been done to choose a transistor which can have better performance in the field of switching devices. In future there is a scope of work to make that converter more usable with a solar system. For example, a constant dc voltage has been used as input for this boost converter, but the solar power supply will not be a constant input system and in this case there will be a scope of work to make the converter usable with a solar system and then shift the voltage level using GaN transistor as a switch.


# Appendix

## FDB2532 Data Sheet



**FDP2532 / FDB2532**  
**N-Channel PowerTrench® MOSFET**  
**150 V, 79 A, 16 mΩ**

October 2013



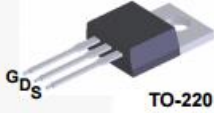
**Features**

- $R_{DS(on)} = 14 \text{ m}\Omega$  (Typ.) @  $V_{GS} = 10 \text{ V}$ ,  $I_D = 33 \text{ A}$
- $Q_{G(tot)} = 82 \text{ nC}$  (Typ.) @  $V_{GS} = 10 \text{ V}$
- Low Miller Charge
- Low  $Q_{rr}$  Body Diode
- UIS Capability (Single Pulse and Repetitive Pulse)

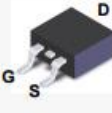
**Applications**

- Consumer Appliances
- Synchronous Rectification
- Battery Protection Circuit
- Motor drives and Uninterruptible Power Supplies
- Micro Solar Inverter

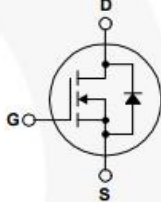
Formerly developmental type 82884



TO-220



D<sup>2</sup>-PAK



**MOSFET Maximum Ratings**  $T_C = 25^\circ\text{C}$  unless otherwise noted

Symbol	Parameter	FDP2532 / FDB2532	Unit
$V_{DSS}$	Drain to Source Voltage	150	V
$V_{GS}$	Gate to Source Voltage	$\pm 20$	V
$I_D$	Drain Current		
	Continuous ( $T_C = 25^\circ\text{C}$ , $V_{GS} = 10\text{V}$ )	79	A
	Continuous ( $T_C = 100^\circ\text{C}$ , $V_{GS} = 10\text{V}$ )	56	A
	Continuous ( $T_{amb} = 25^\circ\text{C}$ , $V_{GS} = 10\text{V}$ , $R_{\theta JA} = 43^\circ\text{C/W}$ )	8	A
	Pulsed	Figure 4	A
$E_{AS}$	Single Pulse Avalanche Energy (Note 1)	400	mJ
$P_D$	Power dissipation	310	W
	Derate above $25^\circ\text{C}$	2.07	W/ $^\circ\text{C}$
$T_J, T_{STG}$	Operating and Storage Temperature	-55 to 175	$^\circ\text{C}$

**Thermal Characteristics**

Symbol	Parameter	FDP2532 / FDB2532	Unit
$R_{\theta JC}$	Thermal Resistance Junction to Case, Max. TO-220, D <sup>2</sup> -PAK	0.61	$^\circ\text{C/W}$
$R_{\theta JA}$	Thermal Resistance Junction to Ambient, Max. TO-220, D <sup>2</sup> -PAK (Note 2)	62	$^\circ\text{C/W}$
$R_{\theta JA}$	Thermal Resistance Junction to Ambient D <sup>2</sup> -PAK, Max. 1in <sup>2</sup> copper pad area	43	$^\circ\text{C/W}$

©2002 Fairchild Semiconductor Corporation  
FDP2532 / FDB2532 Rev. C2

1

www.fairchildsemi.com

FDP2532 / FDB2532 — N-Channel PowerTrench® MOSFET

**Package Marking and Ordering Information**

Device Marking	Device	Package	Reel Size	Tape Width	Quantity
FDB2532	FDB2532	D <sup>2</sup> -PAK	330 mm	24 mm	800 units
FDP2532	FDP2532	TO-220	Tube	N/A	50 units

**Electrical Characteristics**  $T_C = 25^\circ\text{C}$  unless otherwise noted

Symbol	Parameter	Test Conditions	Min	Typ	Max	Unit
--------	-----------	-----------------	-----	-----	-----	------

**Off Characteristics**

$B_{VDS}$	Drain to Source Breakdown Voltage	$I_D = 250\mu\text{A}$ , $V_{GS} = 0\text{V}$	150	-	-	V
$I_{DSS}$	Zero Gate Voltage Drain Current	$V_{DS} = 120\text{V}$ $V_{GS} = 0\text{V}$ $T_C = 150^\circ\text{C}$	-	-	1	$\mu\text{A}$
$I_{GSS}$	Gate to Source Leakage Current	$V_{GS} = \pm 20\text{V}$	-	-	$\pm 100$	nA

**On Characteristics**

$V_{GS(TH)}$	Gate to Source Threshold Voltage	$V_{GS} = V_{DS}$ , $I_D = 250\mu\text{A}$	2	-	4	V
$r_{DS(ON)}$	Drain to Source On Resistance	$I_D = 33\text{A}$ , $V_{GS} = 10\text{V}$	-	0.014	0.016	$\Omega$
		$I_D = 16\text{A}$ , $V_{GS} = 6\text{V}$	-	0.016	0.024	
		$I_D = 33\text{A}$ , $V_{GS} = 10\text{V}$ , $T_C = 175^\circ\text{C}$	-	0.040	0.048	

**Dynamic Characteristics**

$C_{ISS}$	Input Capacitance	$V_{DS} = 25\text{V}$ , $V_{GS} = 0\text{V}$ , $f = 1\text{MHz}$	-	5870	-	pF
$C_{OSS}$	Output Capacitance		-	615	-	pF
$C_{RSS}$	Reverse Transfer Capacitance		-	135	-	pF
$Q_{g(TOT)}$	Total Gate Charge at 10V	$V_{GS} = 0\text{V}$ to 10V	-	82	107	nC
$Q_{g(TH)}$	Threshold Gate Charge	$V_{GS} = 0\text{V}$ to 2V	-	11	14	nC
$Q_{gs}$	Gate to Source Gate Charge	$V_{DD} = 75\text{V}$ $I_D = 33\text{A}$ $I_g = 1.0\text{mA}$	-	23	-	nC
$Q_{gs2}$	Gate Charge Threshold to Plateau		-	13	-	nC
$Q_{gd}$	Gate to Drain "Miller" Charge		-	19	-	nC

**Resistive Switching Characteristics** ( $V_{GS} = 10\text{V}$ )

$t_{ON}$	Turn-On Time	$V_{DD} = 75\text{V}$ , $I_D = 33\text{A}$ $V_{GS} = 10\text{V}$ , $R_{GS} = 3.6\Omega$	-	-	69	ns
$t_{d(ON)}$	Turn-On Delay Time		-	16	-	ns
$t_r$	Rise Time		-	30	-	ns
$t_{d(OFF)}$	Turn-Off Delay Time		-	39	-	ns
$t_f$	Fall Time		-	17	-	ns
$t_{OFF}$	Turn-Off Time		-	-	84	ns

**Drain-Source Diode Characteristics**

$V_{SD}$	Source to Drain Diode Voltage	$I_{SD} = 33\text{A}$	-	-	1.25	V
		$I_{SD} = 16\text{A}$	-	-	1.0	V
$t_{rr}$	Reverse Recovery Time	$I_{SD} = 33\text{A}$ , $dI_{SD}/dt = 100\text{A}/\mu\text{s}$	-	-	105	ns
$Q_{RR}$	Reverse Recovery Charge	$I_{SD} = 33\text{A}$ , $dI_{SD}/dt = 100\text{A}/\mu\text{s}$	-	-	327	nC

**Notes:**

- 1: Starting  $T_J = 25^\circ\text{C}$ ,  $L = 0.5\text{mH}$ ,  $I_{AS} = 40\text{A}$ .  
 2: Pulse Width = 100s



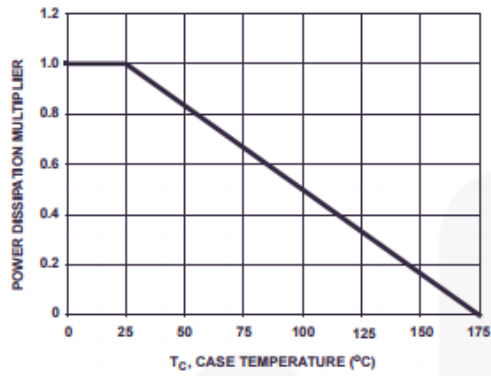


Figure 1. Normalized Power Dissipation vs Ambient Temperature

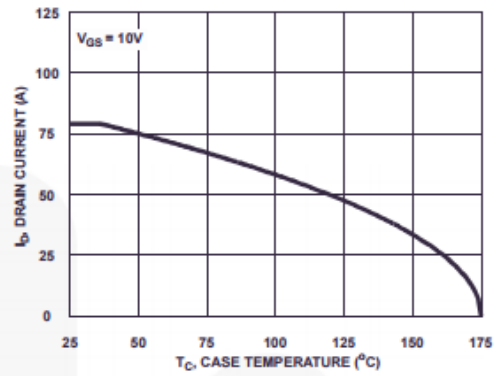


Figure 2. Maximum Continuous Drain Current vs Case Temperature

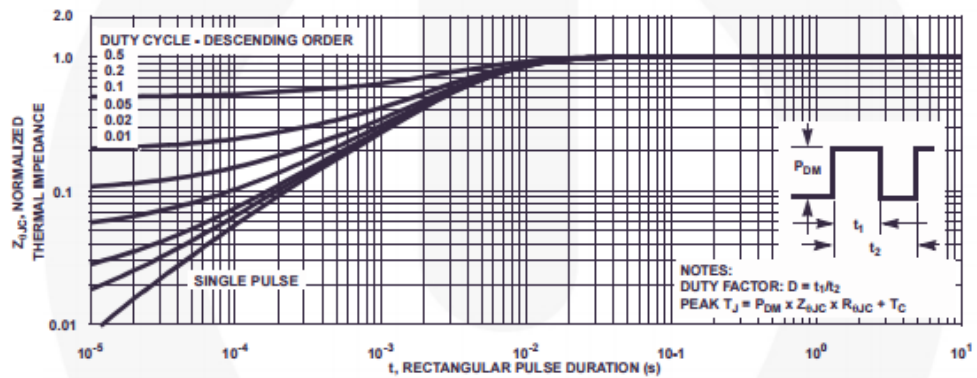


Figure 3. Normalized Maximum Transient Thermal Impedance

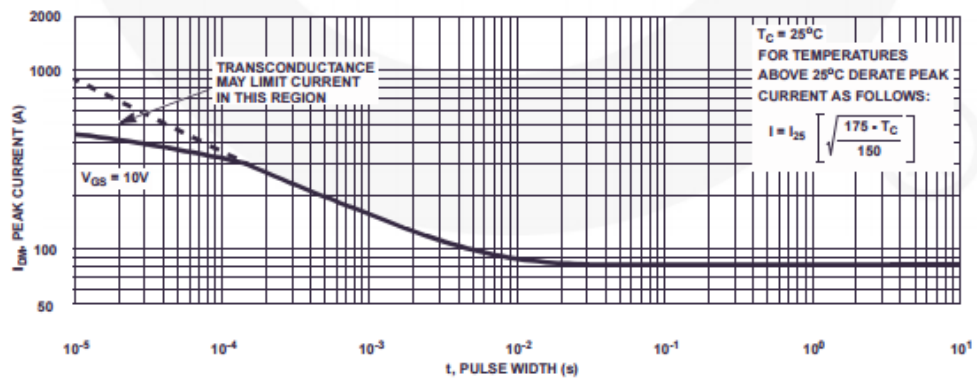
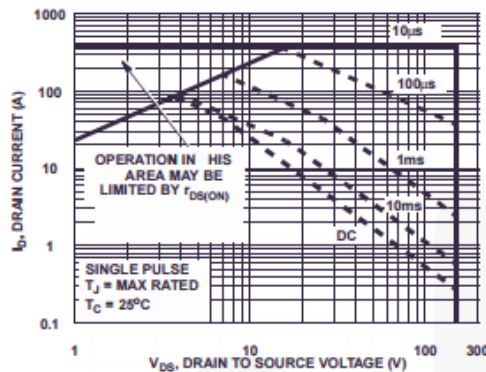
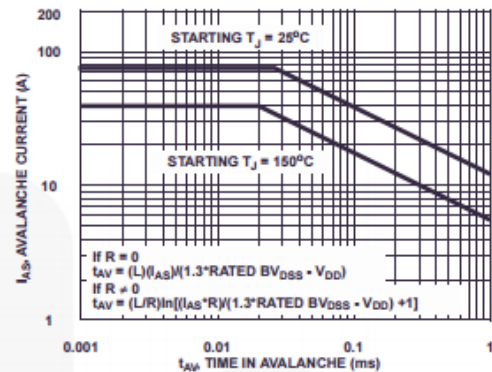
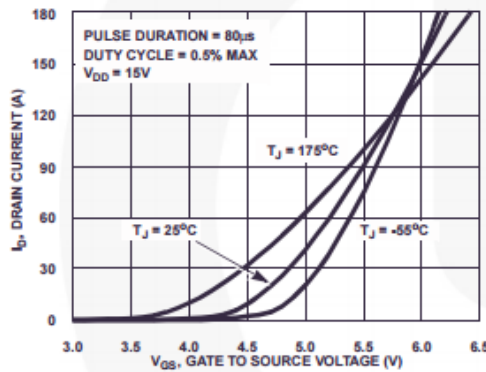
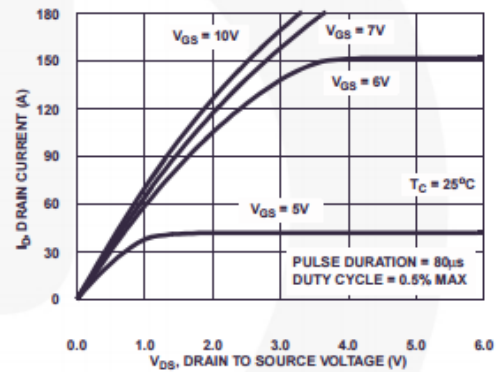
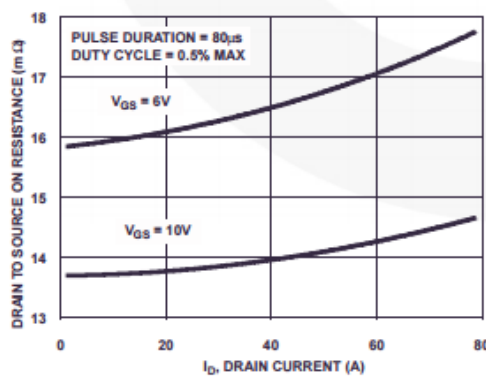
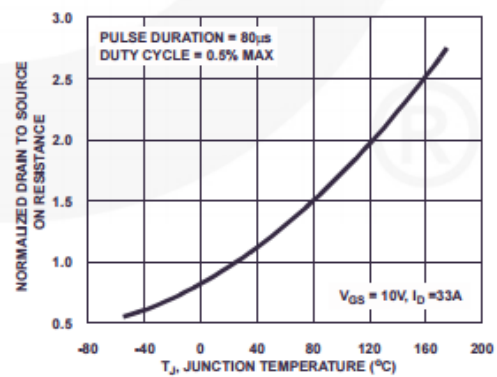


Figure 4. Peak Current Capability

**Typical Characteristics**  $T_C = 25^\circ\text{C}$  unless otherwise noted**Figure 5. Forward Bias Safe Operating Area**

NOTE: Refer to Fairchild Application Notes AN7515 and AN7517

**Figure 6. Unclamped Inductive Switching Capability****Figure 7. Transfer Characteristics****Figure 8. Saturation Characteristics****Figure 9. Drain to Source On Resistance vs Drain Current****Figure 10. Normalized Drain to Source On Resistance vs Junction Temperature**

## EPC2001 Data Sheet

eGaN® FET DATASHEET

EPC2001

EPC2001 – Enhancement Mode Power Transistor

$V_{DSS}, 100\text{ V}$

$R_{DS(ON)}, 7\text{ m}\Omega$

$I_D, 25\text{ A}$

NEW PRODUCT

Halogen-Free

Gallium Nitride is grown on Silicon Wafers and processed using standard CMOS equipment leveraging the infrastructure that has been developed over the last 55 years. GaN's exceptionally high electron mobility and low temperature coefficient allows very low  $R_{DS(ON)}$  while its lateral device structure and majority carrier diode provide exceptionally low  $Q_G$  and zero  $Q_{RR}$ . The end result is a device that can handle tasks where very high switching frequency, and low on-time are beneficial as well as those where on-state losses dominate.

Maximum Ratings			
$V_{DS}$	Drain-to-Source Voltage (Continuous)	100	V
	Drain-to-Source Voltage (up to 10,000 5ms pulses at 125°C)	120	V
$I_D$	Continuous ( $T_A = 25^\circ\text{C}, \theta_{JA} = 13$ )	25	A
	Pulsed (25°C, $T_{pulse} = 300\text{ }\mu\text{s}$ )	100	A
$V_{GS}$	Gate-to-Source Voltage	6	V
	Gate-to-Source Voltage	-5	V
$T_J$	Operating Temperature	-40 to 125	°C
$T_{STG}$	Storage Temperature	-40 to 150	°C

EPC2001 eGaN® FETs are supplied only in passivated die form with solder bars

Applications

- High Speed DC-DC conversion
- Class D Audio
- Hard Switched and High Frequency Circuits

Benefits

- Ultra High Efficiency
- Ultra Low  $R_{DS(ON)}$
- Ultra low  $Q_G$
- Ultra small footprint

PARAMETER	TEST CONDITIONS	MIN	TYP	MAX	UNIT	
<b>Static Characteristics (<math>T_J = 25^\circ\text{C}</math> unless otherwise stated)</b>						
$BV_{DSS}$	Drain-to-Source Voltage	$V_{GS} = 0\text{ V}, I_D = 300\text{ }\mu\text{A}$	100		V	
$I_{DSS}$	Drain Source Leakage	$V_{DS} = 80\text{ V}, V_{GS} = 0\text{ V}$	100	250	$\mu\text{A}$	
$I_{GSS}$	Gate-Source Forward Leakage	$V_{GS} = 5\text{ V}$	1	5	mA	
	Gate-Source Reverse Leakage	$V_{GS} = -5\text{ V}$	0.2	1		
$V_{GS(th)}$	Gate Threshold Voltage	$V_{DS} = V_{GS}, I_D = 5\text{ mA}$	0.7	1.4	2.5	V
$R_{DS(ON)}$	Drain-Source On Resistance	$V_{GS} = 5\text{ V}, I_D = 25\text{ A}$	5.6	7	$\text{m}\Omega$	
<b>Source-Drain Characteristics (<math>T_J = 25^\circ\text{C}</math> unless otherwise stated)</b>						
$V_{SD}$	Source-Drain Forward Voltage	$I_S = 0.5\text{ A}, V_{GS} = 0\text{ V}, T = 25^\circ\text{C}$	1.75		V	
		$I_S = 0.5\text{ A}, V_{GS} = 0\text{ V}, T = 125^\circ\text{C}$	1.8			

All measurements were done with substrate shorted to source.

Thermal Characteristics			
		TYP	
$R_{\theta JC}$	Thermal Resistance, Junction to Case	2.1	°C/W
$R_{\theta JB}$	Thermal Resistance, Junction to Board	15	°C/W
$R_{\theta JA}$	Thermal Resistance, Junction to Ambient (Note 1)	54	°C/W

Note 1:  $R_{\theta JA}$  is determined with the device mounted on one square inch of copper pad, single layer 2 oz copper on FR4 board.  
See [http://epc-co.com/epc/documents/product-training/Appnote\\_Thermal\\_Performance\\_of\\_eGaN\\_FETs.pdf](http://epc-co.com/epc/documents/product-training/Appnote_Thermal_Performance_of_eGaN_FETs.pdf) for details.

EPC – EFFICIENT POWER CONVERSION CORPORATION | [WWW.EPC-CO.COM](http://WWW.EPC-CO.COM) | COPYRIGHT 2013 |

PAGE 1

PARAMETER	TEST CONDITIONS	MIN	TYP	MAX	UNIT
<b>Dynamic Characteristics</b> ( $T_J = 25^\circ\text{C}$ unless otherwise stated)					
$C_{iss}$	Input Capacitance		850	950	pF
$C_{oss}$	Output Capacitance		450	525	
$C_{rss}$	Reverse Transfer Capacitance		20	30	
$Q_G$	Total Gate Charge ( $V_{GS} = 5\text{ V}$ )		8	10	nC
$Q_{GD}$	Gate to Drain Charge		2.2	2.7	
$Q_{GS}$	Gate to Source Charge		2.3	2.8	
$Q_{OSS}$	Output Charge		35	40	
$Q_{RR}$	Source-Drain Recovery Charge		0	0	

All measurements were done with substrate shorted to source.

Figure 1: Typical Output Characteristics

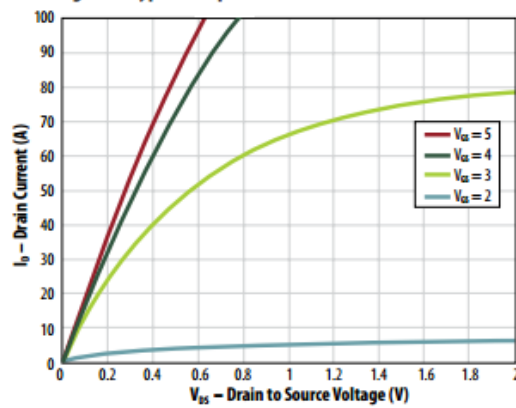


Figure 2: Transfer Characteristics

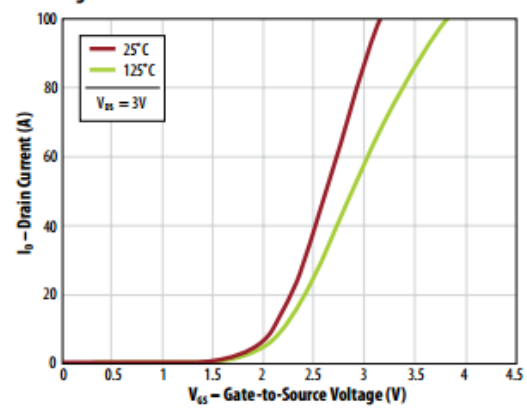


Figure 3:  $R_{DS(on)}$  vs  $V_{GS}$  for Various Current

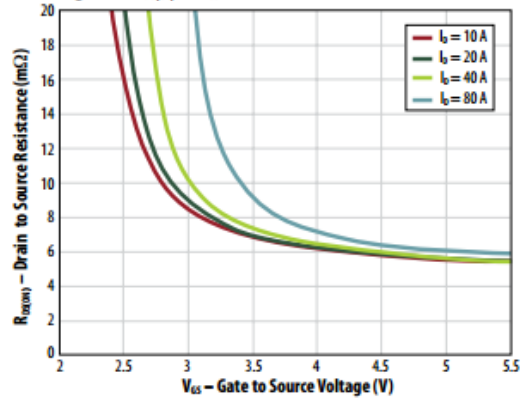


Figure 4:  $R_{DS(on)}$  vs  $V_{GS}$  for Various Temperature

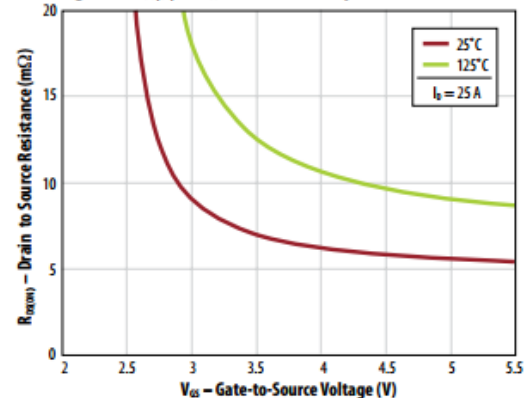


Figure 5: Capacitance

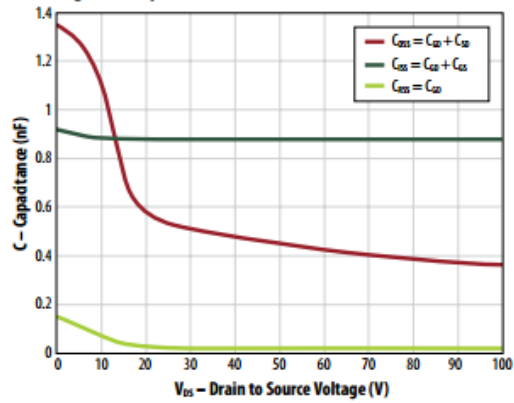


Figure 6: Gate Charge

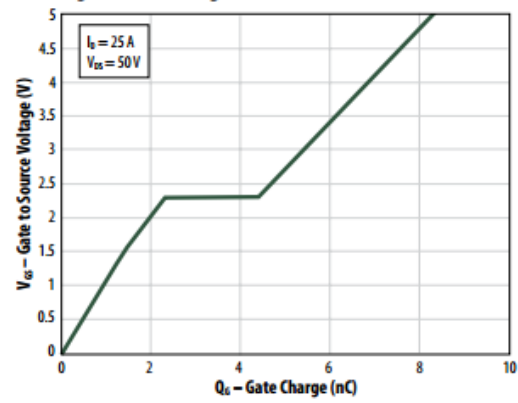


Figure 7: Reverse Drain-Source Characteristics

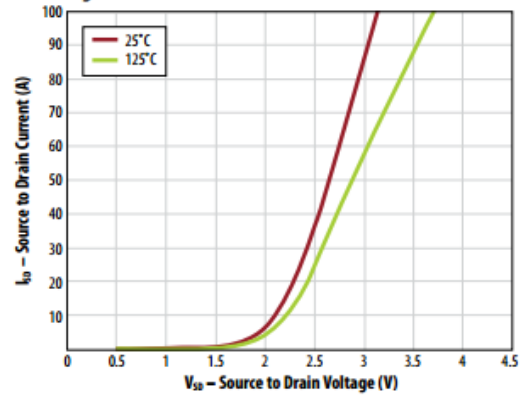


Figure 8: Normalized On Resistance Vs Temperature

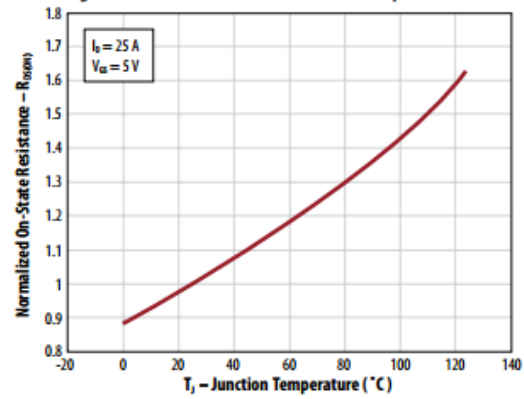


Figure 9: Normalized Threshold Voltage vs. Temperature

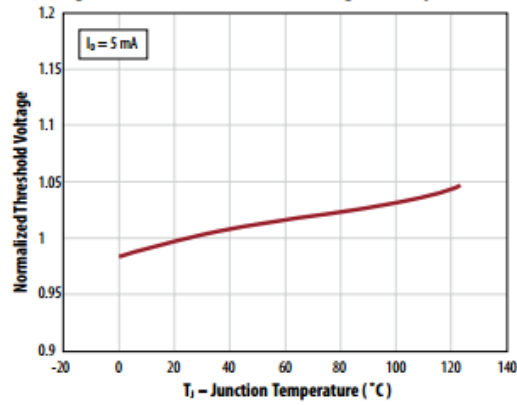
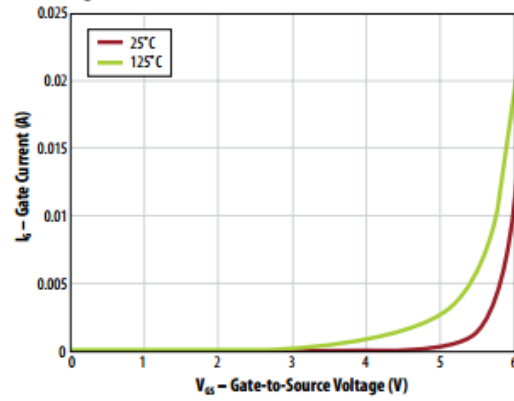


Figure 10: Gate Current



All measurements were done with substrate shorted to source.

## C2M0025120D Data Sheet



## C2M0025120D

Silicon Carbide Power MOSFET

C2M™ MOSFET Technology

N-Channel Enhancement Mode

## Features

- High Blocking Voltage with Low On-Resistance
- High Speed Switching with Low Capacitances
- Easy to Parallel and Simple to Drive
- Avalanche Ruggedness
- Resistant to Latch-Up
- Halogen Free, RoHS Compliant

## Benefits

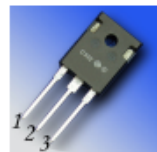
- Higher System Efficiency
- Reduced Cooling Requirements
- Increased Power Density
- Increased System Switching Frequency

## Applications

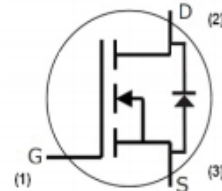
- Solar Inverters
- Switch Mode Power Supplies
- High Voltage DC/DC converters
- Battery Chargers
- Motor Drive
- Pulsed Power Applications

$V_{DS}$	1200 V
$I_D @ 25^\circ\text{C}$	90 A
$R_{DS(on)}$	25 mΩ

## Package



TO-247-3



Part Number	Package
C2M0025120D	TO-247-3

Maximum Ratings ( $T_c = 25^\circ\text{C}$  unless otherwise specified)

Symbol	Parameter	Value	Unit	Test Conditions	Note
$V_{DSmax}$	Drain - Source Voltage	1200	V	$V_{GS} = 0\text{ V}, I_G = 100\text{ }\mu\text{A}$	
$V_{GSmax}$	Gate - Source Voltage	-10/+25	V	Absolute maximum values	
$V_{GSop}$	Gate - Source Voltage	-5/+20	V	Recommended operational values	
$I_D$	Continuous Drain Current	90	A	$V_{GS} = 20\text{ V}, T_C = 25^\circ\text{C}$	Fig. 19
		60		$V_{GS} = 20\text{ V}, T_C = 100^\circ\text{C}$	
$I_{D(pulse)}$	Pulsed Drain Current	250	A	Pulse width $t_p$ limited by $T_{Jmax}$	Fig. 22
$P_D$	Power Dissipation	463	W	$T_c = 25^\circ\text{C}, T_J = 150^\circ\text{C}$	Fig. 20
$T_J, T_{stg}$	Operating Junction and Storage Temperature	-55 to +150	$^\circ\text{C}$		
$T_L$	Solder Temperature	260	$^\circ\text{C}$	1.6mm (0.063") from case for 10s	
$M_d$	Mounting Torque	1 8.8	Nm lbf-in	M3 or 6-32 screw	




**Electrical Characteristics** ( $T_c = 25^\circ\text{C}$  unless otherwise specified)

Symbol	Parameter	Min.	Typ.	Max.	Unit	Test Conditions	Note
$V_{DS(BOSS)}$	Drain-Source Breakdown Voltage	1200			V	$V_{GS} = 0\text{ V}, I_D = 100\text{ }\mu\text{A}$	
$V_{GS(th)}$	Gate Threshold Voltage	2.0	2.6	4	V	$V_{DS} = V_{GS}, I_D = 15\text{ mA}$	Fig. 11
			2.1		V	$V_{DS} = V_{GS}, I_D = 15\text{ mA}, T_J = 150^\circ\text{C}$	
$I_{GSS}$	Zero Gate Voltage Drain Current		2	100	$\mu\text{A}$	$V_{DS} = 1200\text{ V}, V_{GS} = 0\text{ V}$	
$I_{SS}$	Gate-Source Leakage Current			600	nA	$V_{GS} = 20\text{ V}, V_{DS} = 0\text{ V}$	
$R_{DS(on)}$	Drain-Source On-State Resistance		25	34	m $\Omega$	$V_{GS} = 20\text{ V}, I_D = 50\text{ A}$	Fig. 4,5,6
			43			$V_{GS} = 20\text{ V}, I_D = 50\text{ A}, T_J = 150^\circ\text{C}$	
$g_{fs}$	Transconductance		23.6		S	$V_{GS} = 20\text{ V}, I_{DS} = 50\text{ A}$	Fig. 7
			21.7			$V_{GS} = 20\text{ V}, I_{DS} = 50\text{ A}, T_J = 150^\circ\text{C}$	
$C_{iss}$	Input Capacitance		2788		pF	$V_{GS} = 0\text{ V}$	Fig. 17,18
$C_{oss}$	Output Capacitance		220			$V_{DS} = 1000\text{ V}$	
$C_{rss}$	Reverse Transfer Capacitance		15			$f = 1\text{ MHz}$	
$E_{oss}$	$C_{oss}$ Stored Energy		121		$\mu\text{J}$	$V_{AC} = 25\text{ mV}$	Fig 16
$E_{AS}$	Avalanche Energy, Single Pluse		3.5		J	$I_D = 50\text{ A}, V_{DS} = 50\text{ V}$	Fig. 29
$E_{on}$	Turn-On Switching Energy		1.4		mJ	$V_{DS} = 800\text{ V}, V_{GS} = -5/20\text{ V},$ $I_D = 50\text{ A}, R_{G(ext)} = 2.5\Omega, L = 412\text{ }\mu\text{H}$	Fig. 25
$E_{off}$	Turn Off Switching Energy		0.3				
$t_{d(on)}$	Turn-On Delay Time		14		ns	$V_{DS} = 800\text{ V}, V_{GS} = -5/20\text{ V}$ $I_D = 50\text{ A},$ $R_{G(ext)} = 2.5\text{ }\Omega, R_L = 16\text{ }\Omega$ Timing relative to $V_{DS}$ Per IEC60747-8-4 pg 83	Fig. 27
$t_r$	Rise Time		32				
$t_{d(off)}$	Turn-Off Delay Time		29				
$t_f$	Fall Time		28				
$R_{G(int)}$	Internal Gate Resistance		1.1		$\Omega$	$f = 1\text{ MHz}, V_{AC} = 25\text{ mV}, \text{ESR of } C_{iss}$	
$Q_{gs}$	Gate to Source Charge		46		nC	$V_{DS} = 800\text{ V}, V_{GS} = -5/20\text{ V}$ $I_D = 50\text{ A}$ Per IEC60747-8-4 pg 83	Fig. 12
$Q_{gd}$	Gate to Drain Charge		50				
$Q_g$	Total Gate Charge		161				

**Reverse Diode Characteristics**

Symbol	Parameter	Typ.	Max.	Unit	Test Conditions	Note
$V_{SD}$	Diode Forward Voltage	3.3		V	$V_{GS} = -5\text{ V}, I_{SD} = 25\text{ A}$	Fig. 8, 9, 10
		3.1		V	$V_{GS} = -5\text{ V}, I_{SD} = 25\text{ A}, T_J = 150^\circ\text{C}$	
$I_S$	Continuous Diode Forward Current		90		$T_c = 25^\circ\text{C}$	Note 1
$t_{rr}$	Reverse Recovery Time	45		ns	$V_{GS} = -5\text{ V}, I_{SD} = 50\text{ A}, T_J = 25^\circ\text{C}$ $VR = 800\text{ V}$ $di/dt = 1000\text{ A}/\mu\text{s}$	Note 1
$Q_{rr}$	Reverse Recovery Charge	406		nC		
$I_{rrm}$	Peak Reverse Recovery Current	13.5		A		

Note (1): When using SiC Body Diode the maximum recommended  $V_{GS} = -5\text{ V}$

**Thermal Characteristics**

Symbol	Parameter	Typ.	Max.	Unit	Test Conditions	Note
$R_{\theta JC}$	Thermal Resistance from Junction to Case	0.24	0.27	$^\circ\text{C}/\text{W}$		Fig. 21
$R_{\theta JA}$	Thermal Resistance from Junction to Ambient		40			

# References

- [1] D. Costinett, H. Nguyen, R. Zane and D. Maksimovic, "GaN-FET based dual active bridge DC-DC converter," 2011 Twenty-Sixth Annual IEEE Applied Power Electronics Conference and Exposition (APEC), Fort Worth, TX, 2011, pp. 1425-1432. doi: 10.1109/APEC.2011.5744779
- [2] F. Gamand, M. D. Li and C. Gaquiere, "A 10-MHz GaN HEMT DC/DC Boost Converter for Power Amplifier Applications," *in* IEEE Transactions on Circuits and Systems II: Express Briefs, vol. 59, no. 11, pp. 776-779, Nov. 2012. doi: 10.1109/TCSII.2012.2228397
- [3] N. Kaminski and O. Hilt, "SiC and GaN devices - wide bandgap is not all the same," *in* IET Circuits, Devices & Systems, vol. 8, no. 3, pp. 227-236, May 2014. doi: 10.1049/iet-cds.2013.0223
- [4] S.H. Penzin, W.R. Crain, K.B. Crawford, et al., The SEU pulse width modulation controllers with soft start and shutdown circuits. IEEE Radiation Effects Data Workshop, USA, 1993, pp. 73–79.
- [5] F.Y. Shih, Y.T. Chen, D.Y. Chen, et al. A PSpice-compatible model of PWM IC for switching power converters with soft-start characteristic, in: Proceedings of International Conference on Power Electronics and Drive Systems, Singapore, 1995, pp. 335–340.
- [6] A. Hariya, K. Matsuura, H. Yanagi, S. Tomioka, Y. Ishizuka and T. Ninomiya, "Five-Megahertz PWM-Controlled Current-Mode Resonant DC–DC Step-Down Converter Using GaN-HEMTs," *in* IEEE Transactions on Industry Applications, vol. 51, no. 4, pp. 3263-3272, July-Aug. 2015. doi: 10.1109/TIA.2015.2391439
- [7] Z. Zhang, W. Zhang, F. Wang, L. M. Tolbert and B. J. Blalock, "Analysis of the switching speed limitation of wide band-gap devices in a phase-leg configuration," 2012 IEEE Energy Conversion Congress and Exposition (ECCE), Raleigh, NC, 2012, pp. 3950-3955. doi: 10.1109/ECCE.2012.6342164
- [8] Richardson R. F. P. D, "Gallium Nitride (GaN) Vs Silicon Carbide (SiC) in High frequency (RF) and Power Switching applications." Microsemi PPG, pp 1-6.
- [9] "www.cooperindustries.com," cooperindustries, [Online]. Available: [http://www.cooperindustries.com/content/dam/public/bussmann/Electronics/Resources/Brochures/Switching\\_Regulator\\_Inductor\\_Application\\_Guide.pdf](http://www.cooperindustries.com/content/dam/public/bussmann/Electronics/Resources/Brochures/Switching_Regulator_Inductor_Application_Guide.pdf). [Accessed 2017]
- [10] L. G. Grainger and R. C. Spencer, "Residual harmonics in voltage unbalanced power systems," *in* IEEE Transactions on Industry Applications, vol. 30, no. 5, pp. 1398-1405, Sep/Oct1994. doi: 10.1109/28.315254
- [11] "www.epc-co.com," Efficient Power Conversion Corporation [online]. Available: <http://epc-co.com/epc/Products/eGaNfETsandICs/epc2001.aspx>



- [12] A. Hariya, K. Matsuura, H. Yanagi, S. Tomioka, Y. Ishizuka and T. Ninomiya, "Five-Megahertz PWM-Controlled Current-Mode Resonant DC–DC Step-Down Converter Using GaN-HEMTs," in *IEEE Transactions on Industry Applications*, vol. 51, no. 4, pp. 3263-3272, July-Aug. 2015. doi: 10.1109/TIA.2015.2391439
- [13] "www.epc-co.com," Efficient Power Conversion Corporation [online]. Available: <http://epc-co.com/epc/EventsandNews/News/PageID/8/PgrID/1627/PID/2995/TagID/96/TagName/IBS.aspx>
- [14] W. Zhang et al., "Evaluation and comparison of silicon and gallium nitride power transistors in LLC resonant converter," in *Proc. IEEE Energy Convers. Congr. Expo. Conf.*, 2012, pp. 1362–1366.
- [15] D. Reusch and J. Strydom "Evaluation of gallium nitride transistors in high frequency resonant and soft-switching DC–DC converters" *Proc. IEEE Appl. Power Electron. Conf.* pp. 464-470 2014.
- [16] J. Delaine, P. O. Jeannin, D. Frey K. and Guepratte "High frequency DC–DC converter using GaN device" *Proc. IEEE Appl. Power Electron. Conf.* pp. 1754-1761 2012.
- [17] F. Schwier, J. Pezoldt and R. Granzner, "Two-dimensional materials and their prospects in transistor electronics" in *The Royal Society of Chemistry, Journal*, 2015.
- [18] Mariusz Zdanowski, Jacek Rąbkowski, "Operation modes of the GaN HEMT in high-frequency half-bridge converter", *Progress in Applied Electrical Engineering (PAEE)*, pp. 1-6, 2016.
- [19] Onur Esame, Yasar Gurbuz, Ibrahim Tekin and Ayhan Bozkurt, "Performance comparison of state-of-the-art heterojunction bipolar devices (HBT) based on AlGaAs/GaAs, Si/SiGe and InGaAs/InP", in *Microelectronics Journal*, Volume 35 Issue 11, November 2004, Page 901-908
- [20] Jack Browne "What's the difference between GaN and GaAs", MECA Electronics, Inc [online] available: <http://mwrf.com/materials/what-s-difference-between-gan-and-gaas>.
- [21] M. Kuball *et al.*, "Measurement of temperature in active high-power AlGaIn/GaN HFETs using Raman spectroscopy," in *IEEE Electron Device Letters*, vol. 23, no. 1, pp. 7-9, Jan. 2002. doi: 10.1109/55.974795
- [22] R. Negra, T. D. Chu, M. Helaoui, S. Boumaiza, G. M. Hegazi and F. M. Ghannouchi, "Switch-based GaN HEMT model suitable for highly-efficient RF power amplifier design," *2007 IEEE/MTT-S International Microwave Symposium*, Honolulu, HI, 2007, pp. 795-798. doi: 10.1109/MWSYM.2007.380078
- [23] Ke Wang, Li Geng and Qingrui Meng, "Efficiency improvement in buck-boost converter aimed at SOC utilization," *2008 IEEE International Conference on Industrial Technology*, Chengdu, 2008, pp. 1-5. doi: 10.1109/ICIT.2008.4608490
- [24] T. Ishibashi *et al.*, "Experimental Validation of Normally-On GaN HEMT and Its Gate Drive Circuit," in *IEEE Transactions on Industry Applications*, vol. 51, no. 3, pp. 2415-2422, May-June 2015. doi: 10.1109/TIA.2014.2369818
- [25] N. Al-Masood, S. R. Deeba, A. Hasib Chowdhury, Maria Rahman, Sazzar A. Rahman Fahim Hasan, and Md. Jakir Hossain, "Savings of electricity consumption cost in residential sector of Bangladesh," *2011 IEEE 14th International Multitopic Conference*, Karachi, 2011, pp. 159-163. doi: 10.1109/INMIC.2011.6151463

- [26] Jean- Jacques DeLisle, "GaN enables RF where LDMOS and GaAs can't", [online], Available: <http://mwrfl.com/active-components/gan-enables-rf-where-ldmos-and-gaas-cant>
- [27] J. Millan, P. Godignon, X. Perpina, A. Perez-Tomas, J. Rebollo, "A survey of wide bandgap power semiconductor devices," *IEEE Trans. on Power Electronics*, vol. 29, pp. 2155– 2163, May 2014.
- [28] N. Kaminski, "State of the art and the future of wide band-gap devices," in *Proc. 13th European Conference on Power Electronics and Applications*, pp. 1-9, Sep.2009.
- [29] B. J. Baliga, "Semiconductors for high-voltage, vertical channel fieldeffect transistors," *Journal of Applied Physics*, vol. 53, pp.1759-1764, Mar 1982
- [30] R. Ramachandran, M. Nymand, "Design and Analysis of an Ultra-High Efficiency Phase Shifted Full Bridge GaN Converter," *Applied Power Electronics Conference and Exposition, 30th Annual APEC Conference Proceedings 2015*, pp.2011-2016, Mar 2015
- [31] L. Garcia-Rodriguez, V. Jones, J. Balda, E. Lindstrom, A. Oliva and J. Gonzalez-Llorente, "Design of a GaN-based microinverter for photovoltaic systems," 2014 *IEEE International Symposium in Power Electronics for Distributed Generation Systems (PEDG)*, June 2014
- [32] S. Inoue, H. Akagi, "A bi-directional isolated dc/dc converter as a core circuit of the next-generation medium-voltage power conversion system," *IEEE Trans. Power Electron.*, vol. 22, no. 2, pp.535 -542, 2007
- [33] H. J. Chiu, L. W. Lin, "A bidirectional dc-dc converter for fuel cell electric vehicle driving system", *IEEE Trans. Power Electron.*, vol. 21, no. 4, pp.950 -958, 2006
- [34] Y. Miura, M. Kaga, Y. Horita, and T. Ise, "Bidirectional isolated dual full-bridge dc-dc converter with active clamp for EDLC," in *Proc. IEEE Energy Convers. Congr. Expo.* pp. 1036–1143, Sep. 2010
- [35] Rakesh Ramachandran, Morten Nymand "A 98% Efficient bidirectional full bridge isolated dc-dc GaN converter," *Applied Power Electronics Conference and Exposition (APEC) 2016 IEEE*, ISBN 978-1-4673-8394-3
- [36] R. R. Grzybowski, "Advances in electronic packaging technologies to temperatures as high as 500o C," *Proc. High-Temperature Electronic Materials, Devices and Sensor Conf.*, pp. 207-215, 1998.
- [37] C. S. White et al., "High temperature electronic systems using silicon semiconductors," *Proc. IEEE-IAS Annual Meeting*, pp. 967-976, Oct. 1998
- [38] G. Spiazzi et al., "Performance evaluation of a Schottky SiC power diode in a boost PFC application," *IEEE Trans. Power Electronics*, Vol. 18, No. 6, pp. 1249- 1253, Nov. 2003.
- [39] W. Wright et al., "Comparison of Si and SiC diodes during operation in three-phase inverter driving ac induction motor," *Electronic Letters*, Vol. 37, No. 12, pp. 787-788, June 2001.
- [40] Biswajit Ray, Russel L. Spyker, "High Temperature Design and Testing of a DC-DC power converter with Si and SiC Devices". *IEEE*, PP 1261-1266, ISBN: 0-7803-8486-5/04, 2004

- [41] M. S. Hooper, J. W. Hall and S. Kenny, "A 5 MHz silicon CMOS hierarchical boost DC-DC converter design using macromodels for a 1U process," The 2002 45th Midwest Symposium on Circuits and Systems, 2002. MWSCAS-2002., 2002, pp. II-351-II-354 vol.2. doi: 10.1109/MWSCAS.2002.1186870
- [42] W. A. Tabisz, and F. C La., "Zero Voltage Switching Multi-Resonant Technique-A Novel Approach to Improve Performance of High Frequency Quasi. Resonant Converters," 19th Annual IEEE Power Electronics Specialist Conference, Vol. I, pp. 9-11, 1988
- [43] Valtchov V. T. et al, "Design Considerations and loss analysis of ZVS-voltage switching boost converter," Electric Power Applications, IEEE Proceedings. Volume: 148 Issue: Lpp.29 -33, Jan. 2001.
- [44] Bhat A.K.S., Gurun Ulan R., "A Soft Switched Boost Converter for High Frequency Operation," 19th Annual IEEE Power Electronics Specialist Conference. Vol. I, pp. 463-468, 1999
- [45] Minyu Cai , Liyao Wu , Dakshina Murthy-Bellur , Maryam Saeedifard , Oleg Wasynczuk, "Influence of Si/SiC Device Selection on Losses and Magnetics Design in an Isolated DC-DC Converter" Integrated Power Packaging (IWIPP), DOI: 10.1109/IWIPP.2015.7295980, IEEE 2015
- [46] M. Sasagawa, T. Nakamura, H. Inoue, and T. Funaki, "A study on the high frequency operation of DC-DC converter with SiC DMOSFET," Int. Power Electron. Conf. (IPEC), Jun. 2010, pp. 1946-1949
- [47] J. Cho, C. Jeong, and F. Lee, "Zero-voltage and zero-current-switching full-bridge PWM converter using secondary active clamp," IEEE Trans. Power Electron., vol. 13, no. 4, pp. 601-607, Jul 1998.
- [48] A. Pozo Arribas, M. Krishnamurthy, and K. Shenai, "A simple and accurate circuit simulation model for high-voltage SiC power MOSFETs," Electrochem. Soc. Trans. Gallium Nitride Silicon Carbide Power Technol., vol. 64, no. 7, pp. 99-110, Jan. 2014
- [49] L. Wu, J. Qin, M. Saeedifard, O. Wasynczuk, and K. Shenai, "Efficiency Evaluation of the Modular Multilevel Converter Based on Si and SiC Switching Devices for Medium/High-Voltage Applications," IEEE Trans. Electron Dev., vol. 62, no. 2, pp. 286-293, Feb. 2015.
- [50] D. C. Jiles and D. L. Atherton, "Theory of ferromagnetic hysteresis," Journal of Magnetism and Magnetic Materials, vol. 61, no. 1-2, pp. 48- 60, Jan. 1986.
- [51] R. Prieto, J. A. Cobos, O. Garcia, P. Alou, and J. Uceda, "Model of integrated magnetics by means of "double 2D" finite element analysis techniques," 30th Annu. IEEE Power Electron. Spec. Conf., Aug. 1999, pp. 598-603
- [52] J. Biela, M. Schweizer, S. Waffler, and J. W. Kolar, "SiC versus Si— Evaluation of potentials for performance improvement of inverter and DC-DC converter systems by SiC power semiconductors," IEEE Trans. Ind. Electron., vol. 58, no. 7, pp. 2872-2882, Jul. 2011.
- [53] F. Krismer et.al, "Accurate Power Loss Model Derivation of a High Current Dual Active Bridge Converter for an Automotive Application," IEEE Trans. on Industrial Electronics, Vol.57, NO.3 2010

- [54] K. Itoh et al; "Analysis and Design of a Multi-port Converter Using Magnetic Coupling Inductor Technique", ECCE2013, pp. 4713-4718, September 2013,
- [55] M. Ishigaki et al, "A New Isolated Multi-Port Converter Using Interleaving and Magnetic Coupling Inductor Technologies," Applied Power Electronics Conference 2013,
- [56] Fang Z. Peng, et al, "A New ZVS Bidirectional DC-DC Converter for Fuel Cell and Battery Application", IEEE Trans. on power electronics, vol.19, no.1, January, 2014,
- [57] Gautam, D.S. et al, "An Automotive Onboard 3.3-kW Battery Charger for PHEV Application", IEEE Trans. on Vehicular Technology, vol 61, pp.3466-3474, July 2012,
- [58] Krismer, F.; Kolar, J.W., "Accurate Power Loss Model Derivation of a High-Current Dual Active Bridge Converter for an Automotive Application," in Industrial Electronics, IEEE Transactions on, vol.57, no.3, pp.881-891, March 2010
- [59] Yu, Ruiyang; Ho, Godwin Kwun Yuan; Pong, Bryan Man Hay; Ling, B.W.-K.; Lam, J., "Computer-Aided Design and Optimization of High-Efficiency LLC Series Resonant Converter," in Power Electronics, IEEE Transactions on, vol.27, no.7, pp.3243-3256, July 2012
- [60] Hurley, W.G.; Gath, E.; Breslin, J.G., "Optimizing the AC resistance of multilayer transformer windings with arbitrary current waveforms," in Power Electronics, IEEE Transactions on, vol.15, no.2, pp.369-376, Mar 2000
- [61] Suxuan Guo, Xijun Ni, Kai Tan, Huang, A.Q., "Operation principles of bidirectional isolated AC/DC converter with natural clamping soft switching scheme," Industrial Electronics Society, IECON 2014 - 40th Annual Conference
- [62] M. A.G.P, "Applying MiGaN, GaN devices in High Reliability and Space Applications for Maximum Performance and Reliability," 2013. [Online]. Available: [http://www.microsemi.com/documentportal/doc\\_view/132828-ganfet-application-note.pdf](http://www.microsemi.com/documentportal/doc_view/132828-ganfet-application-note.pdf)
- [63] M. Seeman, "GaN Devices in Resonant LLC Converters: System-level considerations," IEEE Power Electron. Mag., vol. 2, no. 1, pp. 36–41, March 2015.
- [64] S. L. Jen, M. T. Peng, C. Y. Hsu, W. H. Chieng, and J. P. Shu, "QuasiResonant Flyback DC/DC Converter Using GaN Power Transistors," World Electric Vehicle Journal, vol. 5, pp. 567–573, 2012.
- [65] Rajender Nune, Anup Anurag, Sandeep Anand, "Comparative Analysis of Power Density in Si MOSFET and GaN HEMT based Flyback Converters" 2016 10th International Conference on Compatibility, Power Electronics and Power Engineering (CPE-POWERENG), Electronic ISSN: 2166-9546, IEEE 2016
- [66] Sataporn Pornpromlikit, Jinho Jeong, Calogero D. Presti, Antonino Scuderi, Peter M. Asbeck, "A Watt-Level Stacked-FET Linear Power Amplifier in Silicon-On-Insulator CMOS," IEEE Trans. Microwave Theory & Tech., Vol.58, No. 1, pp.57-64, January 2010.
- [67] Chaojiang Li, Dawn Wang, Myra Boenke, Ted Letavic, John Cohn, "An Integrated Zigbee Transmitter and DC-DC Converter on 0.18um HV RF CMOS Technology," IEEE 10th International Conference on ASIC, 2013.

- [68] M. Apostolidou, M.P. Vander Heijden, D.M.W. Leenaserts, J. Sonsky, A. Heringa, I. Volokhine, "A 65nm CMOS 30dBm Class-E RF Power Amplifier with 60% Power Added Efficiency," IEEE RFIC Symposium, pp. 141-144, 2008.
- [69] Lars Vestling, Olof Bengtsson and Jorgen Olsson "Enhanced drift in RF-power LDMOS transistors under pulsed stress conditions" IEEE Conference on Microwave, Germany 2010.
- [70] Henglin Chen, Chen Chen, Yuancheng Ren, "Modeling and Characterization of Incomplete Shielding Effect of GND on Common-Mode EMI of a Power Converter", IEEE Transactions on Electromagnetic Compatibility, Aug.2011, 53(3), pp.676-683.
- [71] Datasheet for MBRS140: <http://www.mouser.com/ds/2/149/MBRS140-889579.pdf>